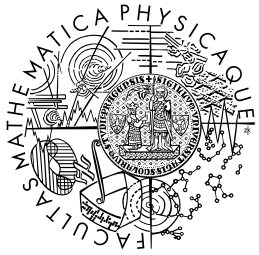

FACULTY
OF MATHEMATICS
AND PHYSICS
Charles University

DOCTORAL THESIS

Jan Kára

Cataclysmic variable stars
Selected borderline systems

Astronomical Institute of Charles University

Supervisor of the doctoral thesis: doc.RNDr. Marek Wolf, CSs.
Co-supervisor of the doctoral thesis: Dr. Sergey Zharikov
Study programme: Theoretical Physics, Astronomy and Astrophysics
Study branch: P4F1

Prague 2023

I declare that I carried out this doctoral thesis independently, and only with the cited sources, literature and other professional sources. It has not been used to obtain another or the same degree.

I understand that my work relates to the rights and obligations under the Act No. 121/2000 Sb., the Copyright Act, as amended, in particular the fact that the Charles University has the right to conclude a license agreement on the use of this work as a school work pursuant to Section 60 subsection 1 of the Copyright Act.

In ..... date ....

Author's signature

The PhD studies were for me a wonderful journey, and even though at some times it was challenging, there were always many people who helped me on the way to which I would like to thank here.

First of all, I would like to thank my supervisor, Marek Wolf, for his help, guidance, and valuable advice during my studies. He always treated me as an equal colleague and it was a pleasure to work with him during my studies. I am also grateful to co-supervisor of my thesis, Sergey Zharikov, whose expertise on cataclysmic variables and his willingness to share it with me were of great help for me.

I spent part of my studies at the European Sothern Observatory in Chile, for which I am very grateful, as my visit there was very inspiring to me and I will always remember it fondly. Therefore, I would like to thank my colleagues I met at ESO, namely my ESO supervisor Linda Schmidtobreick and Anna F. Pala. They devoted a significant amount of their time to our discussions, which was of significant help for me.

I had the pleasure to always work in a friendly environment, for which I would like to thank my colleagues and office mates from the Charles University, especially David Korda, Jaroslav Merc, Kateřina Flanderová, Nela Dvoříková, and many others. And I also would like to thank Sebastian Kurowski and many other colleagues who I met at ESO, who made my stay in Chile enjoyable, even though we spent most of the time there under pandemic restrictions.

Last but not least, I would like to thank my family for always supporting me throughout my life. Thanks to them, I was able to follow my interests in science, without which I could not have written this thesis.

Title: Cataclysmic variable stars

Author: Jan Kára

Institute: Astronomical Institute of Charles University

Supervisor: doc.RNDr. Marek Wolf, CSs., Astronomical Institute of Charles University

Co-supervisor: Dr. Sergey Zharikov, Instituto de Astronomía, Universidad Nacional Autónoma de México

Abstract: Cataclysmic variable stars are semi-detached binary systems consisting of a white dwarf primary star and a late-type secondary star. The secondary star in these systems is overfilling its Roche lobe, which enables a mass transfer to occur between the components. The transferred matter forms an accretion disc around the white dwarf when no strong magnetic field is present. This thesis presents a study of four different cataclysmic variables using light-curve modelling of eclipses and Doppler tomography as the main methods of analysis. The systems selected for the study belong to different subtypes of cataclysmic variables, but all of them exhibit mass-transfer rates which put them close to a border between systems with stable and unstable accretion disc. Although each of the systems studied represents a different type of cataclysmic variables, the presented study shows that they share some common characteristics and that the study of such systems is important for understanding the evolution of cataclysmic variables and the physical processes connected with them.

Keywords: cataclysmic variables, accretion discs, dwarf novae, nova-likes

Contents

Introduction

In ancient times, stars were considered fixed and unchanging components of the night sky. Throughout history, it was, however, shown on numerous examples that stars are not the unvarying sources of light they were thought to be. One such example of the variability of the stellar population was the observation of supernova SN 1572 by Tycho Brahe. And even though it was not the first observation of such an object (see e.g. Stephenson and Clark, 1976; Clark and Stephenson, 1977, 1982, for examples of older observations), it was Tycho Brahe who coined the term nova when he called the newly appeared object 'new star' in *De nova stella* published in 1573. Tycho's Nova was later classified as a Type Ia supernova (Krause et al., 2008), a final stage of the evolution of an interacting binary system.

Today, the term novae, more specifically classical novae, refers to interacting binary systems that exhibit sudden brightening events with an amplitude of several magnitudes. Together with recurrent novae, dwarf novae, nova-likes and magnetic cataclysmic variables, they form a type of variable stars named cataclysmic variable, whose main trait is a transfer of matter between two components of a binary system, which in most of these systems form an accretion disc. The presence of an accretion disc makes cataclysmic variables natural laboratories for the study of the physics of accretion discs and the accretion process. Despite the numerous studies about cataclysmic variables, these systems are not yet fully understood and there are still problems needed to be solved. And while it is necessary to study the whole sample of cataclysmic variables in order to understand this type of stellar systems, it is also important to thoroughly study and analyse individual cases of these variables. This will allow us to create a larger sample of well-described systems, characterise various subclasses of cataclysmic variables, and learn about differences and similarities between these subclasses.

1. Cataclysmic variables

Cataclysmic variables (CVs) are binary systems consisting of a white dwarf as primary and a late-type (K-M) secondary star, which overfills its Roche lobe up to the Lagrangian point L_1. This allows mass to be transferred from the secondary onto the white dwarf, which can happen either via an accretion disc, supposing that the magnetic field of the white dwarf is weak ($< 10^5$ G), or along the magnetic field lines of the white dwarf, when the magnetic field is strong. In systems where the white dwarf has a strong magnetic field, the accretion can be disrupted either partially or entirely and the mass is accreted by the white dwarf alongside its magnetic field lines. The accreting matter can result in sudden increases of brightness by several magnitudes, which are called outbursts and are also the reason why this class of binaries are called 'cataclysmic'. The mechanism of outbursts as well as their characteristic properties can differ among CVs. Therefore, the outbursts and their properties are one of the useful characteristics of CVs that can be used to group them into classes of similar systems. There are several reviews of CVs: a detailed review of this type of variable stars was published by Warner (1995), a more compact book was published by Hellier (2001), and other reviews were presented, for example, by Robinson (1976) and Giovannelli (2008).

1.1 Classification of cataclysmic variables

As photometric observations are usually easily available for CVs, they have been used as the basis to distinguish the different classes, even though sometimes spectroscopic observations are needed to characterise the systems fully. CVs can be divided into classes called classical novae, dwarf novae, recurrent novae, nova-like variables, and magnetic CVs.

1.1.1 Classical novae

Classical novae are CVs with only one recorded outburst. The outbursts can have amplitudes ranging from 6 to 19 magnitudes and in some cases even more. The amplitude of the outbursts is correlated with the decline rate of nova brightness: the brighter the outburst is, the slower the decline. This can be also used to divide the classical novae into sub-classes of slow novae and fast novae. The outbursts of classical novae are caused by thermonuclear runaways of the hydrogen-rich material that gets accreted on the surface of the white dwarf primary. During the outburst, matter from the outer layers of the white dwarf is ejected into the interstellar medium creating a nova shell; an example of an image of a nova shell is shown in Figure 1.1. The masses of the nova shells were estimated by Yaron et al. (2005) to be in the range between $5.3 \cdot 10^{-8}\ M_\odot$ and $6.6 \cdot 10^{-6}\ M_\odot$. As the outbursts of classical novae are not destructive, they can occur repeatedly. However, the recurrence times of most classical novae are estimated to be $\geq 10^4$ yr (Schmidtobreick et al., 2015; Shara et al., 2018).

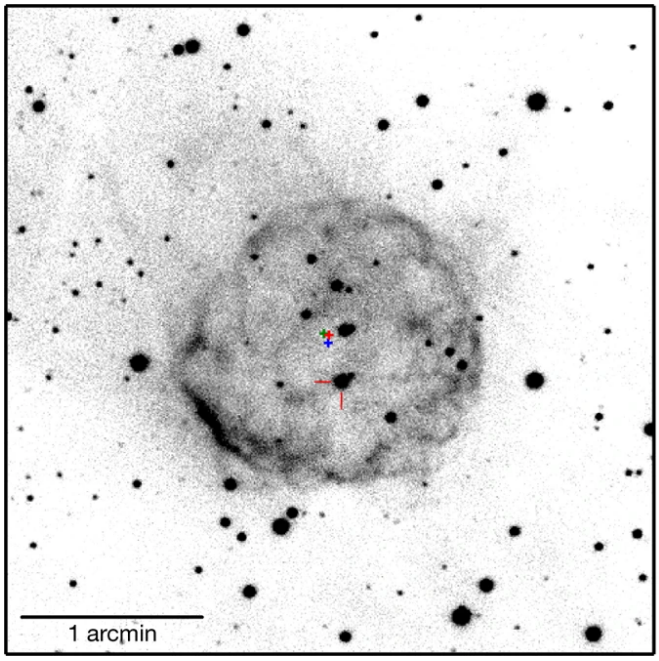

Figure 1.1: The shell associated with Nova Scorpii AD 1437 as presented by Shara et al. (2017). The image was obtained in Hα photometric filter in 2016, the total exposure time is 6 000 s. The red ticks show the position of CV 2MASS J17012815-4306123, the red plus sign shows its estimated position in 1437. The blue plus sign shows the position of the centre on the nova shell, its estimated position in 1473 is marked by the green plus sign.

1.1.2 Dwarf novae

Dwarf novae (DNe) exhibit outbursts, which are smaller in amplitude than the ones of classical novae. Typical amplitudes of DN outbursts are between 1 and 6 magnitudes, and their duration is typically between 2 and 20 days. The outbursts occur semi-regularly with the time intervals between subsequent outbursts ranging typically from several days up to hundreds of days. Unlike the outbursts of classical novae, DN outbursts are caused by the brightenings of the accretion disc. This increase in brightness is caused by a temporary large increase in the mass transfer rate in the accretion disc, which allows for a release of gravitational energy of matter in the disc.

The properties of the outbursts of DNe can be used to group these systems into three separate sub-types: U Gem DNe, SU UMa DNe and Z Cam DNe.

U Gem DNe

U Gem DNe are DNe systems which do not show any characteristics which are peculiar to the DN type. They exhibit outbursts which can differ slightly in shape and duration. An example light curve of a U Gem-type DN is shown in Figure 1.2, top panel. The DN chosen as an example is SS Cyg, which goes through about five outbursts per year.

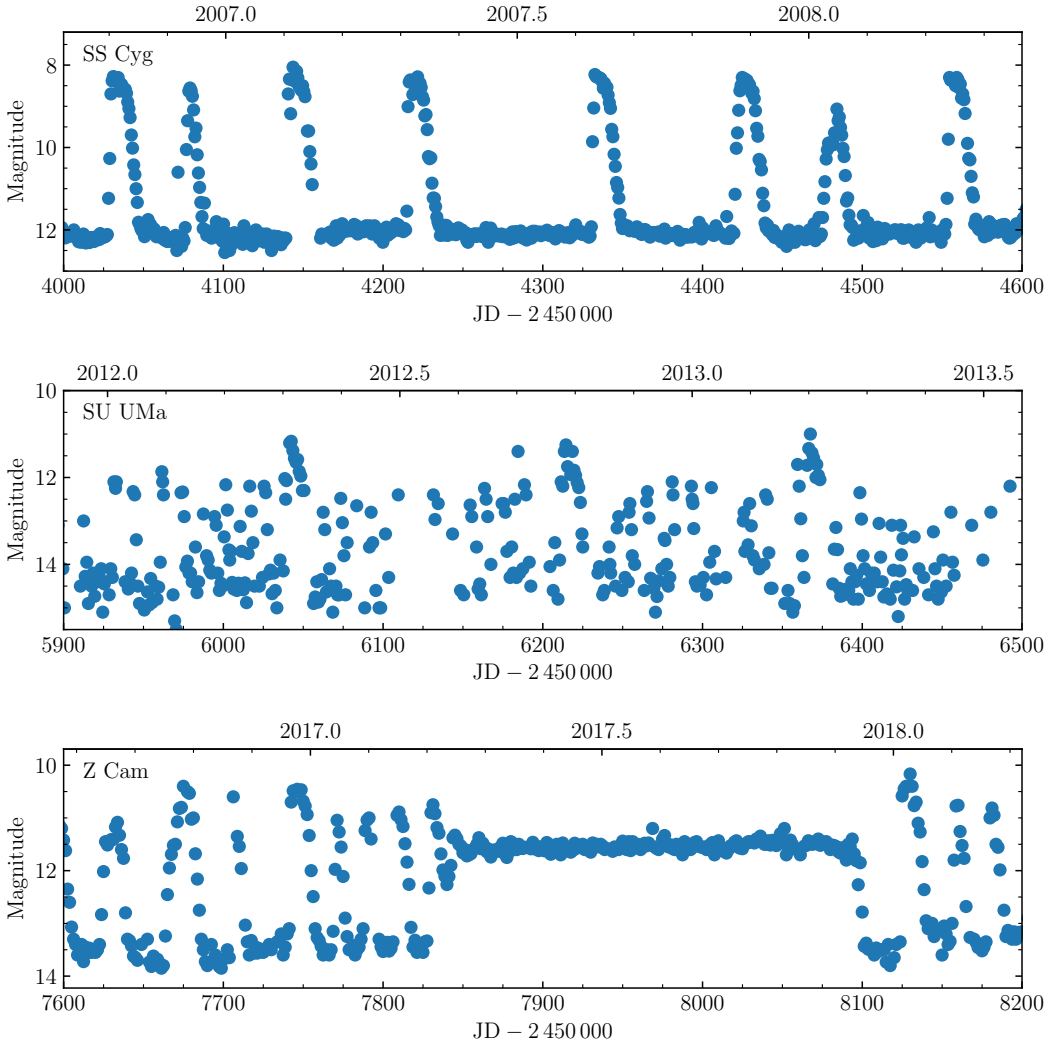

Figure 1.2: Light curves for three DNe, each depicting characteristic behaviour of a different DN sub-type. The light curves show visual magnitudes, data were collected from the database of the American Association of Variable Star Observers (AAVSO, Kloppenborg, 2023).

SU UMa DNe

SU UMa DNe are systems showing two distinct types of outbursts - normal outbursts, similar to the ones of U Gem stars, and superoutbursts, which, compared to the normal outbursts, have about 20% larger amplitude, last longer, and are less frequent in occurrence. An example light curve is shown in the middle panel of Figure 1.2.

Z Cam DNe

While Z Cam systems show DN outbursts similar to U Gem-type stars, the active phase is sometimes interrupted by a standstill, during which the system stays at a constant level of increased brightness, which is, however, less bright than the maximal brightness of the system in an outburst. An example light curve showing both phases of a Z Cam system is shown in the bottom panel of Figure 1.2.

1.1.3 Recurrent novae

Recurrent novae are CVs that went through two and more classical nova outbursts. They can be distinguished from a DN by the ejection of matter from the white dwarf shell during the outbursts, which is not present during DN outbursts.

1.1.4 Nova-like variables

Nova-like variables (NLs) are a subgroup of CVs, which do not show any outbursting activity, but the system clearly consists of a white dwarf and a late-type star overfilling its Roche lobe. NLs can be classical novae for which no outburst has been observed or Z Cam systems in a state of a permanent standstill. One subgroup of NLs, VY Scl stars, show sudden decreases in brightness instead of outbursts, and because of this behaviour, they are sometimes called anti-dwarf novae.

1.1.5 Magnetic cataclysmic variables

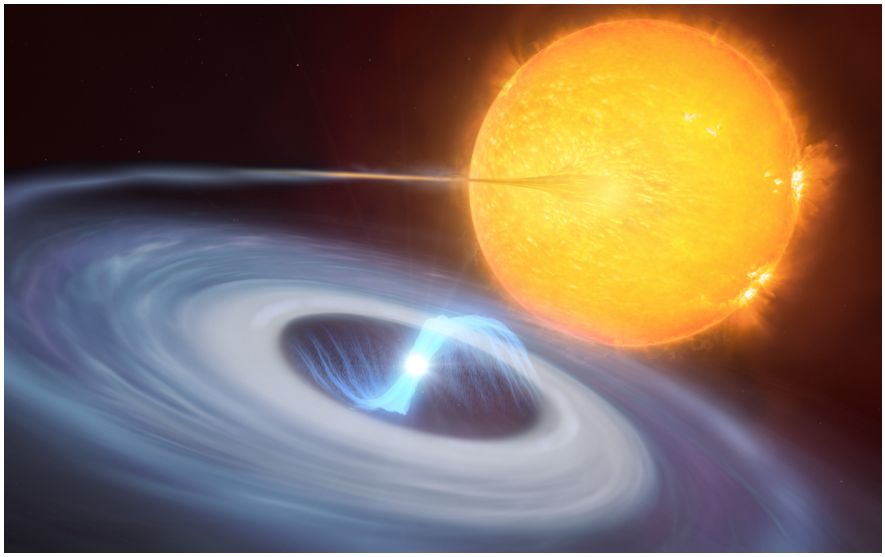

Figure 1.3: Artist's impression of an intermediate polar. Credit: ESO/M. Kornmesser, L. Calçada

Magnetic CVs are systems whose white dwarf has a strong magnetic field, which then controls the accretion process and may disrupt the accretion disc either partially or completely. The systems where the disc is disrupted completely and the transferred material is accreted onto the white dwarf alongside its magnetic field lines are called polars. In systems, when the magnetic field of the white dwarf disrupts the accretion disc only partially, the transferred matter forms a ring around the white dwarf. The matter is then accreted onto the white dwarf from the inner edge of the ring alongside the magnetic field lines. As the accreting matter follows the magnetic field lines, it accretes onto the white dwarf on the magnetic poles of the star. An artistic view of an intermediate polar is shown in Figure 1.3.

Even though magnetic CVs are sometimes included among NLs, some of them exhibit nova outbursts and DN-like outbursts have been reported for several intermediate polars. Recently, Scaringi et al. (2022a,b) observed outbursts of magnetic CVs TV Col, EI UMa, and ASASSN-19bh which they explain as localised runaway events confined by the strong magnetic field. These localised outbursts have a total energy of about 10^{-6} of classical nova outbursts and are called 'micronovae.'

1.1.6 Shortcomings of the classification

The way CVs are classified in their classes has also its shortcomings. In some cases, the classification is governed by the availability of observational data, as the difference between a classical nova and recurrent nova can be created only by an insufficiently long time span for which the system is observed. It is also assumed that all classical novae can be recurrent novae with long recurrence times. Some of the classes of CVs are, however, physically distinct from the other classes, as is, for example, the case of magnetic and non-magnetic CVs. There are also some classical novae which show also DN outbursts. One such system is for example V1017 Sgr (Salazar et al., 2017), which underwent a classical nova outburst in 1919 and three DN outbursts in 1901, 1973 and in 1991. Sometimes, symbiotic novae are also included among CVs. However, the structure of these systems is different from that of a typical CV, as symbiotic binaries are typically detached systems with large orbital periods in the range of hundreds of days (Merc et al., 2019, 2023).

1.2 Physical characteristics

A schematic view of the structure of CV systems is depicted in Figure 1.4, which shows the positions of the most important CV components with respect to the Roche potential of the system. These components are the white dwarf primary, late-type secondary star, an accretion disc, and a bright spot on the accretion disc. Due to the tidal interaction between the secondary and white dwarf, their orbits are circular and the secondary rotates synchronously with the orbital revolution.

As the mass is being transferred from the secondary onto the white dwarf, the secondary becomes smaller, which can lead to subsequent termination of the mass flow when the secondary no longer overfills its Roche lobe. Therefore, in order for the mass transfer to continue, the separation of the stellar component needs to be decreasing over time, which means that CVs need to have a mechanism for decreasing of their angular momentum, which would allow their evolution to smaller separations, i.e. shorter orbital periods.

1.2.1 Orbital period distribution & evolution of cataclysmic variables

CVs are compact systems with orbital periods ranging from about 80 minutes to ~ 10 hours. The distribution of the orbital period is shown in Figure 1.5, which

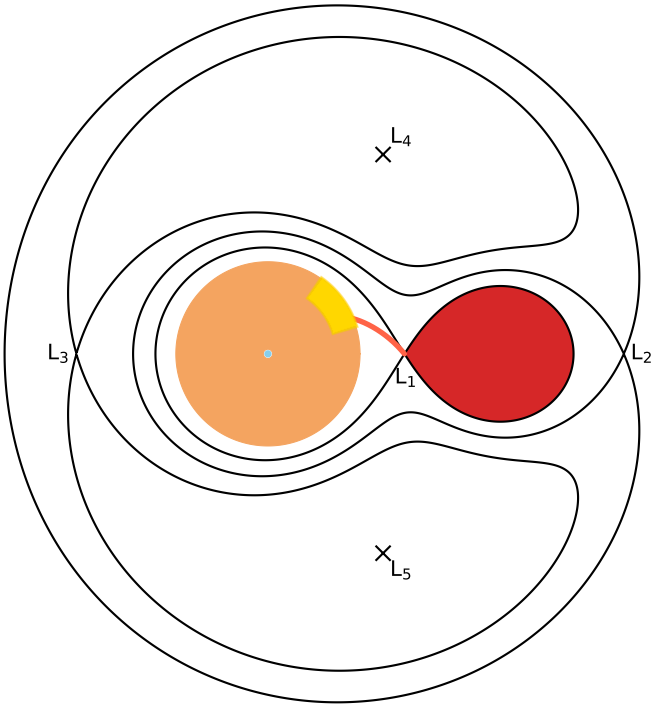

Figure 1.4: Schematic view of a CV with mass ratio $q = \frac{M_2}{M_2} = 0.3$. The black lines represent the equipotentials of a binary system. The secondary (red) fills its Roche lobe up to Lagrangian point L_1 point, through which a matter is transferred via an accretion stream (light red) and accretion disc (light orange) onto the white dwarf (light blue). The place where the accretion stream hits the accretion disc, referred to as bright spot, is marked by yellow.

uses a catalogue of CVs created by Ritter and Kolb (2003, 2004, 2011)[1]. As can be seen in the orbital period distribution, CVs have an orbital period minimum $P_{\min} \sim 80\,\text{min}$ and there is a deficiency in CV systems in the period range between 2 and 3 hours, which is called the period gap. Even though the period minimum is well defined in the orbital period distribution, there is also a number of system with orbital periods bellow 1 hour. These are mostly AM CVn stars, a subclass of helium-rich CVs.

As CVs are evolving towards shorter separation and therefore also towards shorter orbital periods, their angular momentum needs to be decreasing in order for this process to be possible. There are several mechanisms of angular momentum loss which CVs experience throughout their evolution. One of the mechanisms is the radiation of gravitational waves, whose contribution to angular momentum loss $\dot{J}_{\text{GR}}$ is given by formula (Knigge et al., 2011)

$$\dot{J}_{\text{GR}} = -\frac{32}{5}\frac{G^{\frac{7}{2}}}{c^5}\frac{M_1^2 M_2^2 \left(M_1 + M_2\right)^{\frac{1}{2}}}{a^{\frac{7}{2}}}, \tag{1.1}$$

where G is the gravitational constant, c is the speed of light, a is the separation of the stellar components, and M_1 and M_2 are the masses of the primary and

[1] 7th Edition, Release 7.24, February 2017

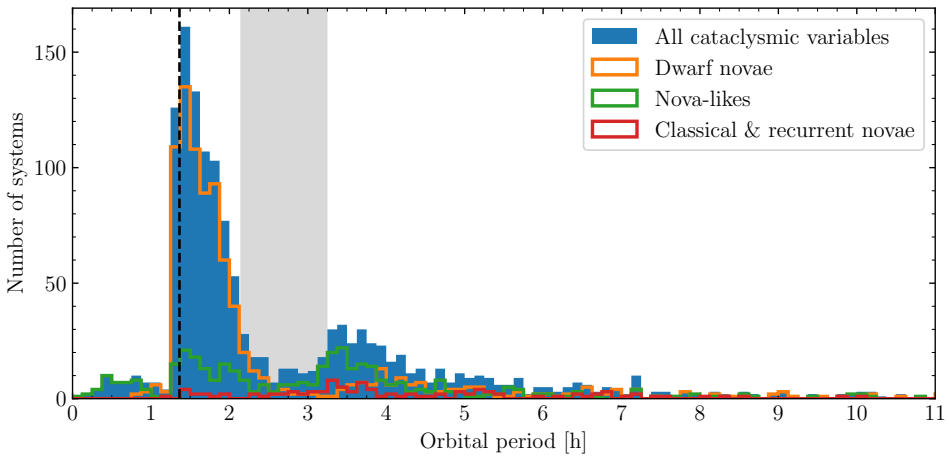

Figure 1.5: Orbital period distribution based on catalogue created by Ritter and Kolb (2003, 2004, 2011). The period minimum and the period gap as predicted by Knigge et al. (2011) are marked by black dashed line and grey area, respectively.

secondary, respectively. However, this mechanism becomes an effective way for angular momentum loss only for orbital periods shorter than ~ 2 hours.

The angular momentum loss of the system with longer orbital periods is expected to be driven by magnetic braking. This way of reducing the angular momentum relies on stellar wind from the secondary, which is forced to co-rotate with the system by the magnetic field of the donor star. During the evolution of CVs, the secondary star becomes fully convective at one point, which results in the vanishing of its magnetic field and subsequent termination of magnetic braking. The donor becomes fully convective in systems with orbital period $P_{\rm orb} \sim 3$ h, at which point the angular momentum loss ceases to be sufficient to drive the mass transfer from the secondary star, and the accretion disc, no longer supplied by matter from the donor, vanishes. As there is no effective way for angular momentum loss in systems with orbital periods between 2 and 3 hours, there is a deficiency of CVs with these orbital periods.

The evolution of orbital period can be described by equation (Knigge et al., 2011)

$$\frac{\dot{P}_{\rm orb}}{P_{\rm orb}} = \frac{3\zeta - 1}{2}\frac{\dot{M}_2}{M_2}, \tag{1.2}$$

where ζ is the mass-radius index defined as

$$\zeta = \frac{{\rm d}\ln R_2}{{\rm d}\ln M_2}. \tag{1.3}$$

For low-mass main-sequence stars, the mass-radius relation can be approximated as $R_2 = M_2^{0.8}$ (Patterson, 1984; Caillault and Patterson, 1990), which gives $\zeta = 0.8$. With $\zeta > \frac{1}{3}$, the orbital period of the CV is decreasing. However, as the mass of the donor is decreasing, the star evolves into a degenerate state in which its size is increasing and the mass-radius index starts to decrease towards value $\zeta = -\frac{1}{3}$ (Rappaport et al., 1982). This means that at some point in their evolution, CVs reach an orbital period minimum $P_{\rm min}$ and after that their orbital period will start to increase. CVs which have passes through the orbital period minimum and

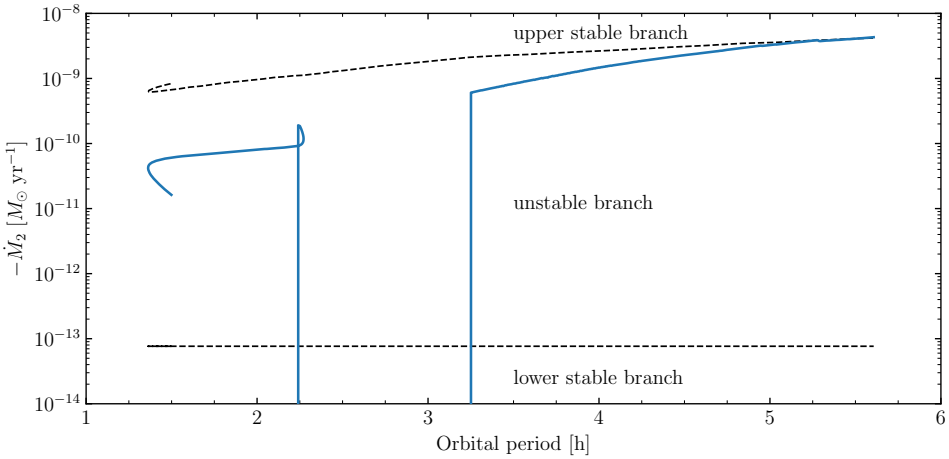

Figure 1.6: Mass loss of the secondary component obtained from the evolutionary model of Knigge et al. (2011). The black lines represent boundaries of the unstable region predicted by thermal disc instability model.

are evolving towards the longer orbital periods are called period bouncers. Large fraction of the galactic CVs is expected to be period bouncers, the evolutionary model of Knigge et al. (2011) predicts this fraction to be 77%. However, CVs which have been identified as period bouncers or suitable candidates form only a small fraction of the know CVs (see e.g. Patterson, 2011; Uthas et al., 2011; Neustroev et al., 2017; Pala et al., 2018; Amantayeva et al., 2021).

Figure 1.6 shows the mass loss of the secondary component predicted by an evolutionary model of Knigge et al. (2011) and its connection to the orbital period. One can clearly see the edges of the period gap and the presence of a period minimum. The period gap in this model occurs for periods between 2.15 and 3.24 hours and the period minimum is predicted to be $P_{\rm min} = 81.8 \pm 0.9$ min. Figure 1.6 also shows the expected boundaries of unstable branch, in which the CVs are expected to undergo the DN outbursts. NLs are expected to have mass-transfer rate in the upper stable branch, in which the accretion disc are in a constant high state. The evolutionary model predicts that CVs can have mass-transfer rate high enough to become NLs for orbital periods larger than $P_{\rm orb} \approx 5$ h, which would mean that most of the CVs with orbital periods above the period gap should be unstable, i.e. DNe. This is, however, not true, as can be seen in Figure 1.5, which shows that NLs dominate the population of CVs with orbital period just above the period gap. A possible explanation for this inconsistency is, that the models of angular momentum loss are not complete and other mechanisms might contribute to it, which would increase the mass-transfer rate. Among the suggested additional mechanisms of angular momentum loss are for example combination of two dynamos responsible for magnetic braking (Zangrilli et al., 1997), or long-term fluctuations of mass-transfer rate (Knigge et al., 2011). Another possible way of reducing the angular momentum is outflow of matter from the system, which was observed in several high-mass transfer NLs (Hernandez et al., 2017; Subebekova et al., 2020; Hernández et al., 2021). Evidence for outflow from the system was observed also in systems AY Psc, SDSS J154453.60+255348.8 (hereafter SDSS1544), and IX Vel, which are discussed in Chapter 3.

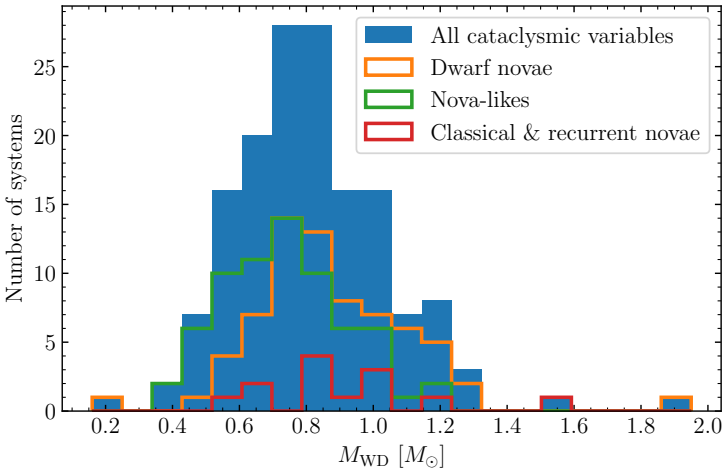

Figure 1.7: White dwarf mass distribution based on Ritter and Kolb (2003, 2004, 2011).

1.2.2 Mass distribution

Although the average mass of single white dwarfs is $\langle M_{\rm WD} \rangle \simeq 0.6\ M_\odot$ (Kepler et al., 2007), binary population studies predict that the average mass of white dwarfs in CVs should be smaller, about $\langle M_{\rm WD} \rangle \simeq 0.5\ M_\odot$ (Politano, 1996; Zorotovic and Schreiber, 2020). However, the observed mass distribution of white dwarfs in CVs shows that their average mass is actually higher than that of single white dwarfs. Figure 1.7 shows the white dwarf mass distribution for 154 CVs from the catalogue created by Ritter and Kolb (2003)[2], the average mass of these white dwarfs is $\langle M_{\rm WD} \rangle = 0.81 \pm 0.18\ M_\odot$. The mass distribution of white dwarfs in CVs was also recently studied by Pala et al. (2022), who analysed a sample of 89 CVs with accurate mass measurements and derived an average mass $\langle M_{\rm WD} \rangle = 0.81^{+0.16}_{-0.20}\ M_\odot$. CVs analysed by Pala et al. (2022) also do not show any dependence of the white dwarf mass on the orbital period of the system, suggesting that the masses of the white dwarfs do not change significantly during the evolution of the CVs.

The discrepancy between the observed average mass of the white dwarfs and the one predicted by evolutionary models is one of the unsolved problems of CV evolution. One possible solution for this problem was suggested by Schreiber et al. (2016), who proposed an additional mechanism of angular momentum loss which would act alongside the magnetic braking and gravitational radiation. The additional mechanism is called consequential angular momentum loss and it is assumed to be more effective for systems with white dwarf of lower masses. The consequential angular momentum loss can cause the mass transfer in the low-mass

[2]The distribution shows two CVs above the Chandrasekhar mass limit. The more massive one is the DN CH UMi whose $M_{\rm WD} = 1.95 \pm 0.03\ M_\odot$ was derived by Friend et al. (1990) under the assumption that the secondary can be considered a main-sequence star. This might have led to an overestimation of the masses of both components. The other system above the Chandrasekhar limit is the recurrent nova U Sco with $M_{\rm WD} = 1.55 \pm 0.24\ M_\odot$ derived by Thoroughgood et al. (2001) from the radial velocities of both components and the duration of the primary eclipse. When taking the uncertainties into account, the mass of the white dwarf can be below the Chandrasekhar limit. Nevertheless, it is still close to the limit, and U Sco is therefore one of the best known candidates for a type Ia supernova among the CVs.

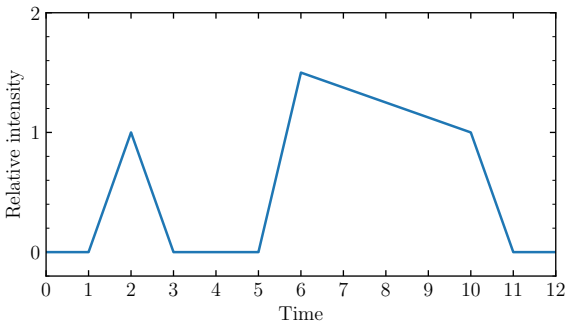

Figure 1.8: Schematic view of the shape of a normal outburst followed by a long outburst.

system to be dynamically unstable and thus it can reduce the number of CV with low-mass white dwarfs.

1.2.3 Accretion disc variability

Outbursts

Although DN outbursts are recurrent events, they are not strictly periodic, and a single system can exhibit outbursts of different properties. Figure 1.8 shows a schematic view of the morphology of light curves of outbursts. The light curve of an outburst typically consists of a rise from quiescence to a maximal brightness, which is then followed by a decline to the original quiescence level. These outbursts are sometimes referred to as normal outbursts. Some outbursts, however, show a plateau phase after reaching their maximum, during which they stay almost at the same brightness level, only with a small decline. These outbursts are called long outbursts and in the case of SU UMa DNe, where the difference between the two types of outbursts is most striking, they are called superoutbursts. There are several empirical relations describing correlation between different properties of outbursts; many possible correlations were analysed by Otulakowska-Hypka et al. (2016), who studied outbursts of DNe of various types.

Thermal disc instability

The generally accepted model that describes the physics of outbursts is the thermal disc instability model, which was suggested by Hōshi (1979), in which the accretion disc oscillates between two stable states with different temperatures. For the accretion disc to undergo outbursts, the mass-transfer rate needs to be between two critical values, in the so-called unstable branch; the relation between the critical mass-transfer rates and the orbital period of the system can be seen in Figure 1.6. When the mass-transfer rate is higher than the upper critical value, the disc stays in a constant high-temperature state, which is the case of NLs. This can be seen in Figure 1.9, which shows the comparison of the measured CV mass transfer rates and the upper critical mass-transfer rate based on the data presented by Dubus et al. (2018). Most of the NLs shown in this figure have mass-transfer rate above or close to the upper boundary of the stable branch.

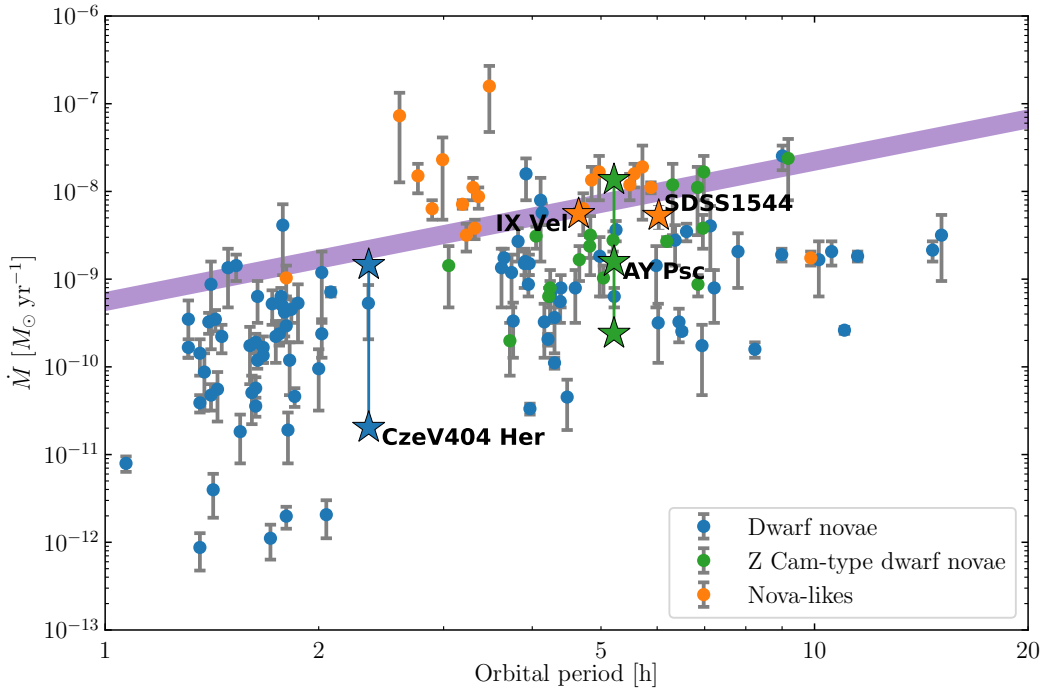

Figure 1.9: Mass-transfer rates of CVs and their orbital periods in comparison to the upper critical mass-transfer rate (purple line) as presented by Dubus et al. (2018). The CV discussed in Chapter 3 are marked by star symbols and labelled. The properties of IX Vel are the ones given by Dubus et al. (2018), properties of CzeV404 Her, AY Psc, and SDSS1544 were adopted from Kára et al. (2021), Kára et al. (2023b), and Medina Rodriguez et al. (2023), respectively. As the mass-transfer rates of CzeV404 Her and AY Psc were derived for different activity states, all derived values are shown. In case of CzeV404 Her, the values correspond to mass-transfer rates in quiescence and during an superoutburst, in case of AY Psc they correspond to quiescence, standstill, and an outburst.

The thermal disc instability model has been used to successfully model many characteristics of the long-term activity of CVs (see e.g. Smak, 1984; Hameury et al., 1998; Cannizzo et al., 2010). The outbursts predicted by this model can originate as instabilities that onset either in the outer regions of the disc or in the inner regions, which results in two types of outburst, as is also observed for DNe, and can account for both normal outbursts and superoutbursts of SU UMa CVs.

Several modifications to the thermal disc instability model were proposed for CVs. One of such models is the thermal-tidal instability model, which takes into account tidal instability caused by the 3:1 resonance between the material in the disc and the orbital motion of the secondary (Whitehurst, 1988; Osaki, 1989, 2005). Due to the tidal forces, the 3:1 resonance causes the disc to become elliptical, which produces additional features in the light curves called superhumps. The superhumps are not observed at a fixed orbital phase, as the elliptical disc precesses, causing the superhumps to appear with a period that is typically slightly longer than the orbital period. In this model, superoutbursts are expected to be the result of the tidal instability, and normal outbursts are explained as the result of the thermal disc instability.

Another proposed model is the enhanced mass-transfer model (Vogt, 1983; Osaki, 1985; Lasota et al., 1995), which assumes that the superoutburst are result of an increased mass-transfer rate from the secondary, which is caused by irradiation of the secondary by the white dwarf and the boundary layer of the accretion disc. Kotko et al. (2012) applied this model to explain the activity of AM CVn stars, a group of hydrogen-poor CVs of short orbital periods, and they concluded that the enhanced mass-transfer is the determining component in the model, which controls the properties of outbursts in these systems. Both the thermal-tidal disc instability model and the enhanced mass-transfer instability model were tested and compared in several studies, e.g. by (Ichikawa et al., 1993; Schreiber et al., 2004). Smak (2008, 2009a,c,d,b) uses observations of Z Cha and other SU UMa stars as evidence that the superoutbursts are caused by enhanced mass-transfer rate and that the superhumps are not caused by eccentricity of the accretion disc, but rather they are caused by dissipation of the gravitational energy of the accretion stream.

Flickering

Another type of variability present in the accretion discs is flickering, which is a phenomenon commonly associated with the accretion process. Flickering is a stochastic low-amplitude variability on a timescale of seconds and minutes. It can originate dominantly in two regions of the accretion disc: in the bright spot and in the inner parts of the accretion disc (see e.g. Bruch, 2000). However, Baptista and Bortoletto (2004, 2008) showed that the sources of flickering can form more complex structures within the disc and that different mechanisms can be responsible for flickering in different parts of the disc. It is also important to note that the accretion disc is not the only possible source of flickering, as flickering was also observed in polars (Iłkiewicz et al., 2022).

2. Observations and methods

2.1 Observations

As in any scientific field, observations are essential for the study of CVs. Characterisation of CVs can make use of photometric and spectroscopic observations, and in the ideal case it combines the two. Due to the complex behaviour of CVs, the observations need to cover various time scales: The analysis of long-term activity requires observation that spans time intervals from several weeks to several years. On the other hand, characterisation of the system and its components usually requires observations that sample the orbital period of the system. With orbital periods of CVs typically below ~ 10 hours, the potential setups for the observations are limited, especially when choosing the exposure time of individual observations. The analyses presented in this work make use of data sets obtained from various facilities and surveys. This chapter presents a summary of the observational data analysed in this work.

2.1.1 Photometry

The photometric data used in the presented research consist of newly obtained data from various observatories and data obtained from various photometric surveys. The main purpose of the newly obtained photometry was to obtain a series of well-sampled light curves covering the eclipses of the selected systems, which allowed us to study time variations in the eclipse occurrence and to model the eclipses in various stages of DN activity. Although these observations can also be used to track the long-term activity of CVs, the distribution of the observing nights only rarely allowed us to have an even coverage over a long period of time. Therefore, we used observations from various photometric surveys to study the long-term activity, since these data sets usually consist of several measurements per night evenly distributed over a long period of time, up to several years.

Mayer 0.65-m telescope

The Mayer 0.65-m telescope (D65) is located at the Ondřejov Observatory in the Czech Republic. It is a reflecting telescope with a focal length of 2342 mm and is equipped with a MI G2-3200 CCD camera. The resolution of the camera is 2184×1472 pixels and the field of view is $19.0' \times 12.8'$.

D65 is regularly used for observations of variable stars, including CVs; e.g. Pilarčík et al. (2012) used D65 to study the period changes of the DN EX Dra. Figure 2.1, left, shows examples of light curves of the DN EX Dra obtained in 2018 in various stages of activity. The presented work makes use of the photometry obtained with this telescope in the analysis of CzeV404 Her (Chapter 3.1), AY Psc (Chapter 3.2), and SDSS1544 (Chapter 3.3).

Danish 1.54-m telescope

The Danish 1.54-m telescope (DK154) is located at the La Silla Observatory in Chile and is equipped with the Danish Faint Object Spectrograph and Camera

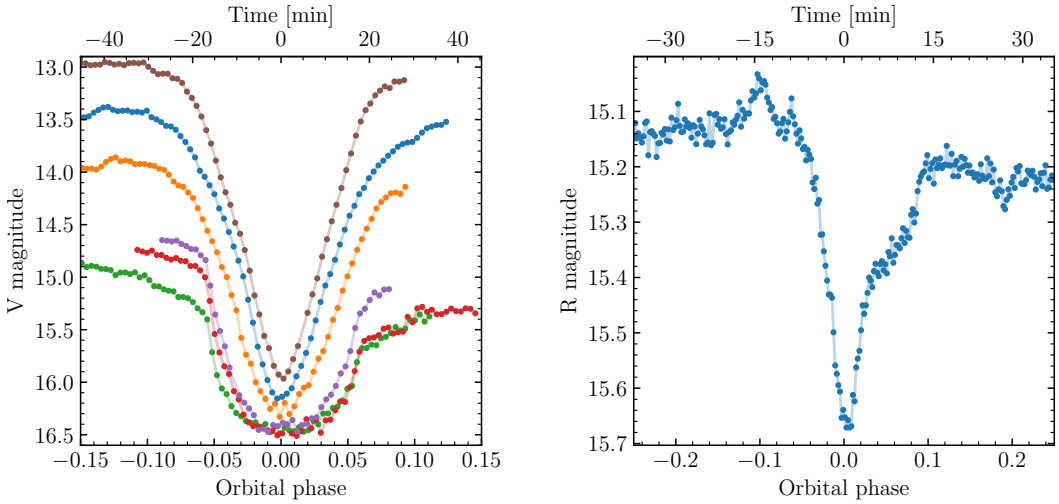

Figure 2.1: *Left:* Examples of light curves of eclipses of EX Dra in different stages of DN activity. The observations were obtained with the D65 telescope at the Ondřejov Observatory throughout 2018 with exposure time of 60 s. *Right:* Light curve of an eclipse of CzeV404 Her obtained with the DK154 at the La Silla Observatory. The data were obtained on March 16, 2019 with exposure time of 7 s.

(DFOSC). However, the spectrograph of DFOSC was decommissioned in 2004 and since then is the instrument used solely for photometry (Skottfelt et al., 2015). The resolution of the DFOSC camera is 2048×2148 pixels, including overscan, and in combination with DK154 offers a field of view of $13.7' \times 13.7'$.

Due to its large aperture, DK154 is suitable for the acquisition of CV light curves with short exposure times down to several seconds. An example light curve is presented in Figure 2.1, right, which shows an eclipse of the DN CzeV404 Her obtained with an exposure time of 7 s. Observations of CVs obtained at this telescope were also used by Pilarčík et al. (2018) to study the changes of orbital periods of three DNe - V2051 Oph, OY Car, and Z Cha. In the presented work, DK154 data were used in the analysis of CzeV404 Her (Chapter 3.1), and AY Psc (Chapter 3.2)

OAN SPM 0.84-m telescope

The 0.84 telescope is located at the Observatorio Astronómico Nacional (OAN) at the San Pedro Mártir Observatory (SPM) in Mexico. The photometry obtained at this telescope was used, e.g., by Amantayeva et al. (2021) to analyse the period bouncer CV EZ Lyn. The presented work uses photometry from this telescope in the analysis of CzeV404 Her (Chapter 3.1), AY Psc (Chapter 3.2), and SDSS1544 (Chapter 3.3).

TESS

Transiting Exoplanet Survey Satellite (TESS; Ricker et al., 2014) is a space telescope designed primary for search of exoplanets transits. Due to its continuous light curves, which cover about $\sim$ 30 days for each observed target, TESS is

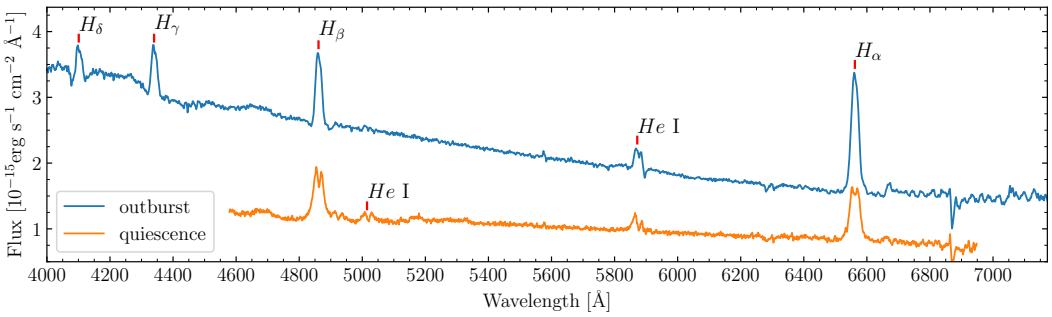

Figure 2.2: Average spectra of CzeV404 Her obtained at SPM Observatory on 2019, April 8 during an outburst and on 2019, July 29 during quiescence phase.

also suitable for study of CVs. Its fast 2 minute cadence mode can be used for eclipse-timing studies as well as for the study of average eclipse profiles in different stages of activity.

Photometric surveys

Several photometric surveys have been used in this work to construct light curves suitable for studying the long-term behaviour of the selected targets. These surveys are the All-Sky Automated Survey (ASAS; Pojmanski, 1997), the All-Sky Automated Survey for Supernovae (ASAS-SN; Shappee et al., 2014; Kochanek et al., 2017), the Zwicky Transient Facility (ZTF; Masci et al., 2019), and the database of the American Association of Variable Star Observers (AAVSO; Kloppenborg, 2023). Examples of light curves showing long-term activity of DNe based on AAVSO observations are shown in Figure 1.2.

2.1.2 Spectroscopy

The spectroscopic data used in the analysis presented in this work were obtained at the SPM Observatory in Mexico and at the La Silla Observatory in Chile. Spectra of CVs covering a wide spectral range can be used to characterise the components of the system, as each component tends to dominate different spectral ranges. The donor, a late-type star, dominates the red and infrared (IR) parts of the spectra, the white dwarf dominates the blue and ultraviolet (UV) parts, and the accretion disc is prominent in the optical and UV ranges. The spectra of accretion discs also contain emission lines, most prominently the hydrogen and helium emission lines. Because the shape of these lines is defined by the properties of the disc, they can be used to study the disc and its structure. For such analysis, a time-resolved series of spectra is needed. The spectra do not need to cover a large spectral range, as only the range focused on a specific line is analysed. As the brightness of the accretion disc varies due to outbursts, so does the spectrum of the CVs. It is therefore advantageous to obtain observations in different phases of activity, which then allows us to study the systems at different stages.

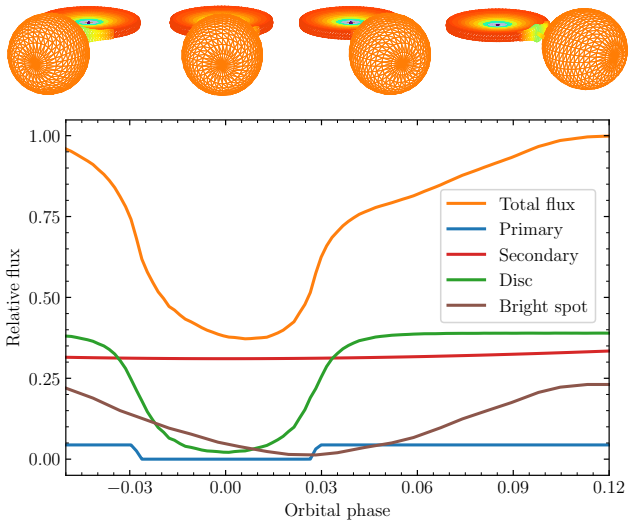

Figure 2.3: Model of the eclipse of AY Psc showing contributions of individual components of the model as presented by Kára et al. (2023b). Geometrical models of the system as viewed during the eclipse are shown above the panel.

OAN SPM 2.12-m telescope

The spectra used in the analysis of CzeV404 Her (Chapter 3.1), AY Psc (Chapter 3.2), and SDSS1544 (Chapter 3.3) were obtained with the 2.12 telescope at SPM Observatory equipped with the Boller and Chivens spectrograph. Mainly two different setups of the instrument were used for the observations, one for acquisition of spectra covering the optical range ($4000 - 7000$ Å) and another for acquisition of spectra covering a smaller spectral range (~ 1200 Å) centred on the Hα line. Figure 2.2 shows example spectra obtained with the 2.21-m telescope.

ESO 3.6-m telescope

The primary data set of spectra used for the analysis of IX Vel (Chapter 3.4) were obtained with the ESO 3.6 equipped with the HARPS spectrograph. The spectra cover the optical spectral range ($3800 - 6900$ Å) with a resolution power of about $R = 80\,000$.

2.2 Methods

2.2.1 Eclipse light-curve modelling

Modelling of eclipse light curves of binary systems is a well-known method which can be used to determine many of their properties. A widely used code for modelling eclipses was presented by Wilson and Devinney (1971), another notable code for eclipse modelling is PHOEBE (Prša and Zwitter, 2005; Prša et al., 2016; Conroy et al., 2020). However, these codes consider only systems where the two stellar components are the only components determining the shape of eclipses. The eclipses of CVs can have more complex shapes determined not only by the

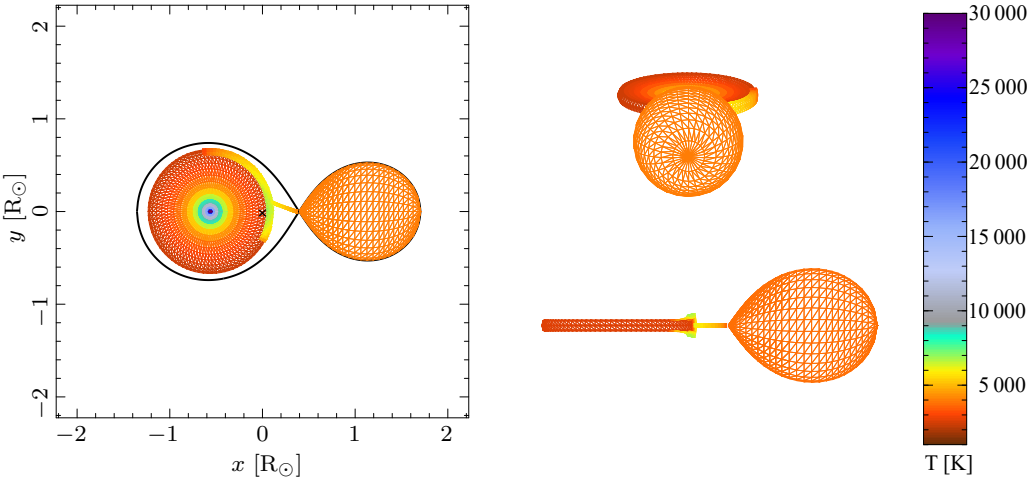

Figure 2.4: Model of AY Psc in the quiescence as presented by Kára et al. (2023b). *Left:* A top-down view showing the geometry of the model. *Right:* Configuration of the system during the primary eclipse at orbital phase $\varphi = 0$ (*top*), and edge-on view of the system corresponding to orbital phase $\varphi = 0.25$ and inclination angle $i = 90°$.

two stellar components, but also by the accretion disc and the hot spot, as can be seen in Figure 2.3.

In this work, we used the code developed by Zharikov et al. (2013) which is based on the code by Wilson and Devinney (1971). A detailed description of the code was presented by Subebekova et al. (2020), Kára et al. (2021, Chapter 3.1 in this work), and Kára et al. (2023b, Chapter 3.2 in this work). In addition to the two stellar components, the model used in this work includes a disc and a bright spot, which contribute to the total flux of the system. An example of the geometry of the model is shown in Figure 2.4, which shows the model of AY Psc in quiescence discussed in Chapter 3.2. The temperature distribution in the disc $T_{\rm eff}(r)$ follows the temperature distribution of the steady-state disc given by

$$\begin{aligned} T_{\rm eff}(r) &= T_* \left[\left(\frac{r}{R_{\rm WD}} \right)^{-3} \left(1 - \left(\frac{R_{\rm WD}}{r} \right)^{\frac{1}{2}} \right) \right]^{EXP}, \\ T_* &= \left(\frac{3GM_{\rm WD}\dot{M}}{8\pi\sigma R_{\rm WD}^3} \right)^{\frac{1}{4}}, \end{aligned} \tag{2.1}$$

where r is the distance from the white dwarf, $R_{\rm WD}$ is the radius of the white dwarf, $\dot{M}$ is the mass-transfer rate and σ is the Stefan-Boltzmann constant. The parameter EXP is in the case of a standard steady-state disc equal to $\frac{1}{4}$ (Warner, 1995, equation 2.35), but during the modelling it is allowed to vary, similarly as was done by Linnell et al. (2010). This allows the temperature distribution in the disc differ from the steady-state disc. The height of the disc $z_{\rm d}$ is defined by equation

$$z_{\rm d} = z_{\rm d,out} \left(\frac{r}{r_{\rm d,out}} \right)^{\gamma_{\rm d}}, \tag{2.2}$$

where $z_{\rm d,out}$ is the height of the disc at the outer edge, $r_{\rm d,out}$ is the distance of the outer edge from the white dwarf, and $\gamma_{\rm d}$ is a parameter defining the radial

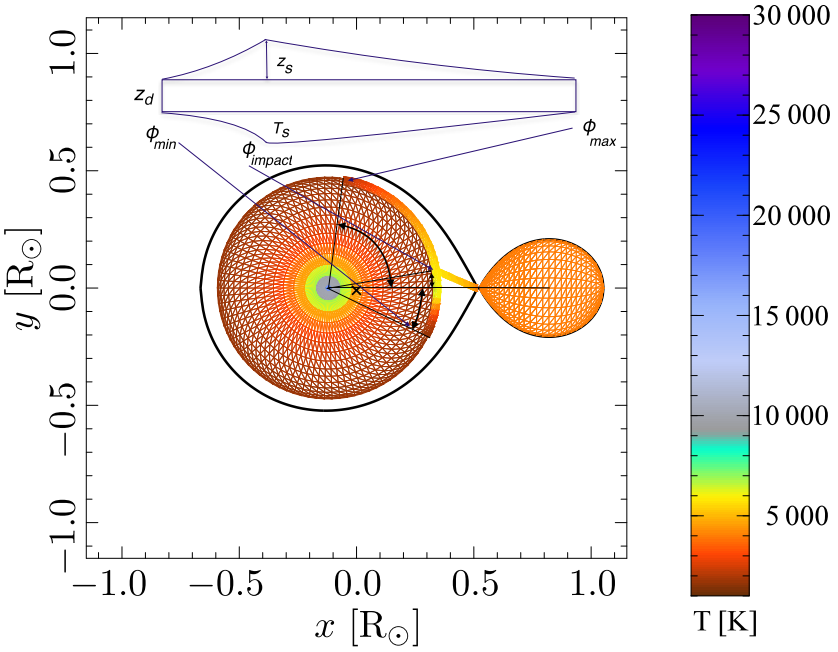

Figure 2.5: Model of CzeV404 Her including the definition of the hot-spot parameters.

dependency of the height of the disc, which in case of a steady-state disc is $\gamma_\mathrm{d} = \frac{9}{8}$ (Warner, 1995, equation 2.51b).

The surface of the accretion disc is divided into a series of triangular elements and the temperature of each element $T_{\mathrm{eff},i}$ is determined using Equation 2.1. The contribution of each element to the observed flux is then calculated as radiation of a black body with temperature $T_{\mathrm{eff},i}$.

The bright spot, the place where the accretion stream intersects with the accretion disc, is included as a separate object. The height z_s and temperature $T_{\mathrm{eff,s}}$ distribution of the bright spot are not uniform. Both distributions have a maximum at the impact point and their decline is modelled by equations

$$z_{\mathrm{s},i}(\phi) = z_\mathrm{d}\left(1 + \gamma_{z,i} f\left(\phi\right)^{\alpha_{z,i}}\right), \tag{2.3a}$$

$$T_{\mathrm{eff,s},i}(\phi) = T_{\mathrm{eff,d}}\left(1 + \gamma_{T,i} f\left(\phi\right)^{\alpha_{T,i}}\right), \tag{2.3b}$$

where ϕ is the angular distance from the impact point, i is an index which distinguishes the part of spot in front of impact point from the part behind impact point, $f\left(\phi\right)$ is a linear function chosen in such way, that $f\left(\phi\right) = 1$ at the impact point and $f\left(\phi\right) = 0$ at the edges of the bright spot, and γ_z, γ_T, α_z and α_T are free parameters.

The best parameters of the model are determined by the gradient descent method. The range of the orbital phase used for fitting is chosen in a way that minimises the effects of flickering originating in the accretion disc, which is strongest outside of the eclipse.

2.2.2 Radial velocities

Determining the radial velocities of the stellar component in CVs is usually not a straightforward process, as the accretion disc usually outshines absorption lines

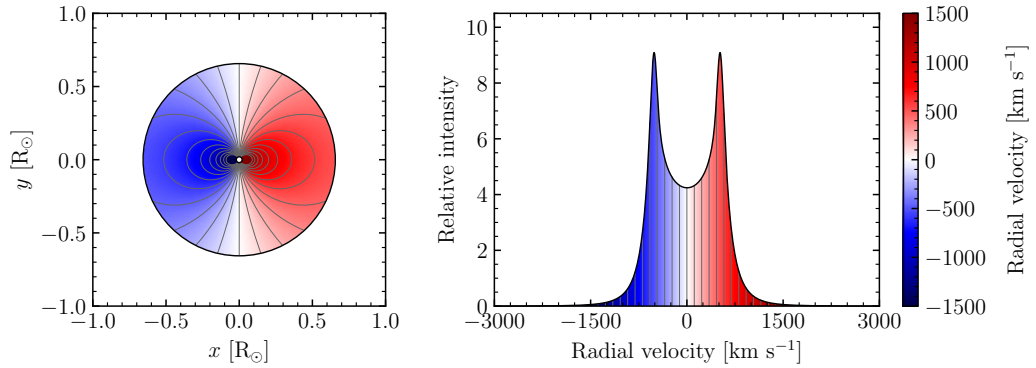

Figure 2.6: Schematic view of the radial velocity distribution of an accretion disc and a resulting emission line originating in such disc. The grey lines connect places of the same radial velocity.

of the white dwarf and the donor star. In cases where absorption lines of the secondary component are observed, they can be used to measure radial velocities. However, these velocities are not representative of the velocity of the centre of mass of the star. The absorption components are weaker on the side of the secondary that faces the primary as a result of irradiation by the white dwarf and the accretion disc. Therefore, the velocities are skewed to larger values. To obtain velocities that describe the motion of the centre of mass, the irradiation of the secondary needs to be taken into account, as demonstrated, e.g., by Wade and Horne (1988); Southworth et al. (2009). In some CVs, the emission lines can originate on the irradiated face of the secondary. These can also be used to determine the radial velocities of the secondary star, but, similarly to the previous case, these velocities also do not reflect the motion of the centre of mass. As the emission comes only from the proximity of the Lagrangian point L_1, the velocities are lower than the velocity of the centre of mass and need to be corrected for this effect, as was shown, e.g., by Beuermann and Thomas (1990); Longa-Peña et al. (2015)

Because the radial velocities of the white dwarf can rarely be measured directly, they are usually inferred from the radial velocities of the accretion disc, which is centred on the white dwarf and follows the same orbital motion. The Doppler shift of the emission lines originating in the disc can be used to determine the radial velocity of the white dwarf.

2.2.3 Spectra of accretion discs

The shape of the emission lines originating in the disc is determined by the velocity distribution of the matter in the accretion disc orbiting the white dwarf. If we assume that the matter in the disc orbits the white dwarf on circular orbit, then the velocity distribution follows the Keplerian velocity $v_{\mathrm{K}} = \sqrt{\frac{G M_1}{r}}$. Figure 2.6, left, shows the projection of the Keplerian velocity distribution in a disc in line of sight with the assumption that the disc is viewed edge on. The right panel of Figure 2.6 then shows the shape of an emission line originating in the disc, if we assume that the emission intensity is the same throughout the disc. However, that is not always the case. The disc can show some radial asymmetry in the

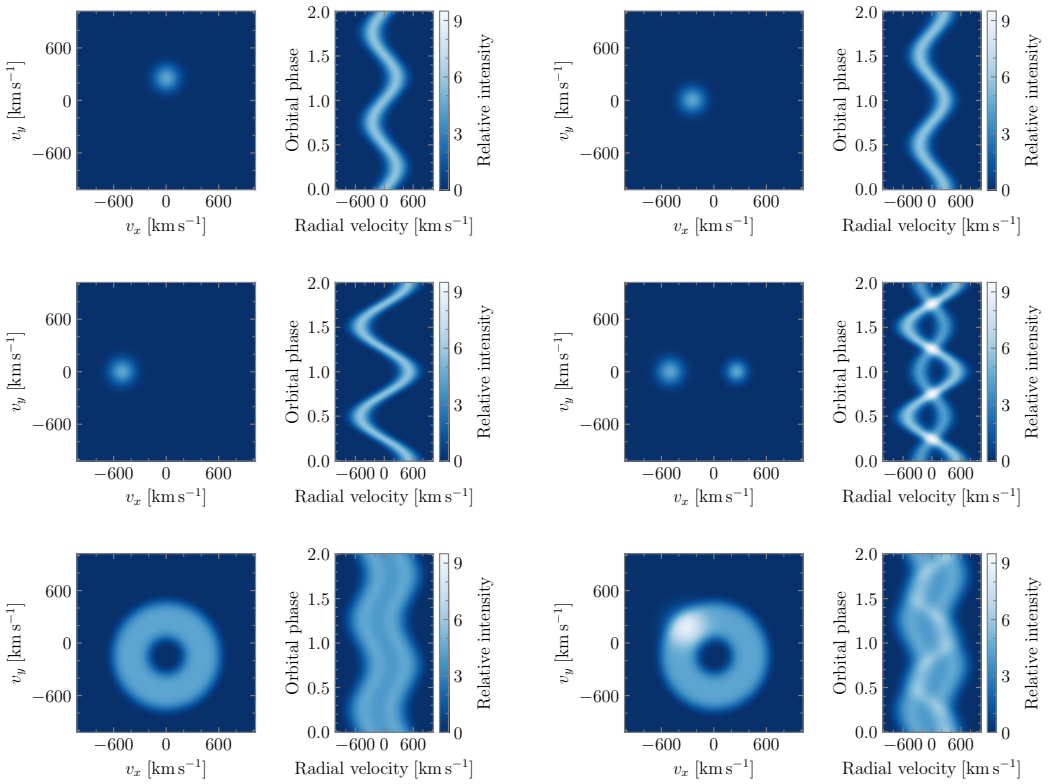

Figure 2.7: Model cases of Doppler maps and corresponding trailed spectra.

density and the temperature distribution, e.g. the bright spot.

When asymmetric features are confined to the outer parts of the disc, as is the case with the bright spot, they affect the shape of the line only in the central parts. It is then possible to use the wings of the line to track the orbital motion of the disc and, by that, the orbital motion of the white dwarf. This can be done by employing a double-Gaussian method described by Schneider and Young (1980); Shafter (1983); Tappert et al. (2003), which uses a weight function consisting of two Gaussians to measure the radial velocities in different parts of the line. However, even this method can be affected by the asymmetric brightness distribution in the disc. Hessman (1987) showed, that the radial velocity curves derived from the wings can show phase shifts up to $\sim 60°$. And also the radial velocities of the system and the amplitudes of the white dwarf velocity curve determined from different emission lines can differ, as was shown , e.g., by Ratering et al. (1993) in the case of the DN KT Per.

CVs with optically thick accretion disc offer an additional opportunity of measuring their radial velocities, as the spectra of thick disc exhibit absorption lines which can be used for these measurements. A CV which shows such absorption lines is, e.g., IX Vel, which is discussed in Chapter 3.4.

2.2.4 Doppler tomography

One method of studying the structure of the accretion discs in CVs is Doppler tomography, which was developed by Marsh and Horne (1988). This method uses time-resolved spectroscopic observations of emission lines originating in the

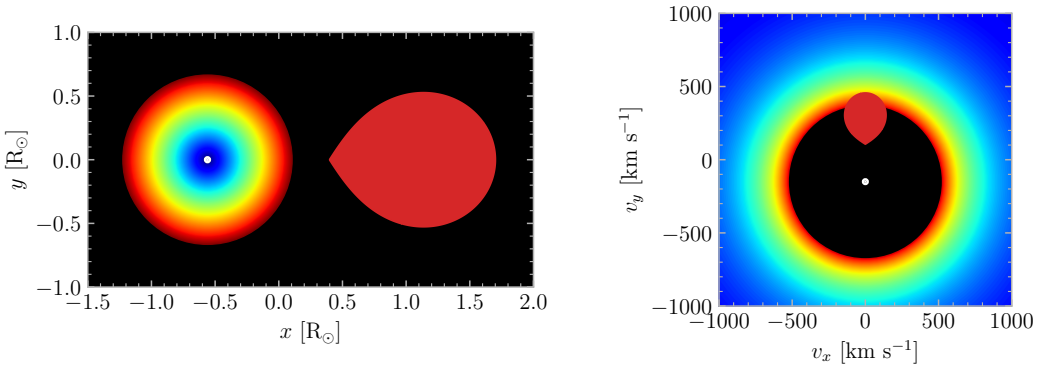

Figure 2.8: Schematic view of a CV in spatial coordinates (*left*) and in velocity coordinates (*right*). The position of the white dwarf is marked by white circle.

accretion disc to reconstruct a map showing the intensity of the emission line in velocity coordinates (v_x, v_y). The method relies on the fact that as the CV orbits its centre of mass, we can observe the system from various angles, which affects the shape of the emission lines due to the different projection of their velocities into the line of sight. Figure 2.7 shows how emission originating at different velocity coordinates affects the shape of the trailed spectra. Each point source of emission creates a sine curve in the trailed spectra, whose amplitude depends on the distance from the centre of mass, and the phase shift of the sine curve is defined by the angular position of the source.

The trailed spectrum can be viewed as a projection of a Doppler map, and it is possible to use a back-projection and the trailed spectrum to obtain the corresponding map. However, this can produce artefacts on the Doppler map, as this method does not take uncertainties into account. It is therefore beneficial to use other methods of deriving the Doppler maps from the observed spectra. In this work, we use a code for Doppler tomography developed by Spruit (1998, 2021), which uses the maximum entropy method to compute the Doppler maps. This method converts the problem of computing the map to a problem of maximising the quantity $\mathcal{Q}$ defined as

$$\mathcal{Q} = \mathcal{H}\left(\vartheta, \tilde{\vartheta}\right) + \alpha\mathcal{S}\left(\psi\right), \tag{2.4}$$

where ψ is the Doppler map, ϑ is the reconstructed spectrum, $\tilde{\vartheta}$ is the observed spectrum, $\mathcal{H}$ is a likelihood which maximises when $\vartheta = \tilde{\vartheta}$, $\mathcal{S}$ is entropy which maximises when the map is smooth, and α is a parameter controlling the importance of the entropy $\mathcal{S}$. A detailed description of this method was presented by Spruit (1998).

Interpreting Doppler maps is not always a straightforward problem, because they represent the emission in the system in velocity coordinates (v_x, v_y). While the velocity distribution in the accretion disc can be assumed to be Keplerian and it would therefore be possible to transform the maps into spatial coordinates (x, y), there can be emission features not related to the accretion disc whose position in the spatial maps would be misleading. Figure 2.8 shows how a map of a CV in spatial coordinates relates to a Doppler map of the same system. It can be clearly seen that on the Doppler map, the secondary overlaps with the outer edge of the

accretion disc. The figure also illustrates that Doppler maps show the accretion disc 'inside-out,' as the outer parts of the disc are found closer to the centre of the map (at low velocities), and the inner parts of the disc are located further from the centre (at high velocities). A detailed review of Doppler tomography and its applications was presented by Marsh (2005).

3. Individual systems

This chapter presents four papers, each of which is a study of an individual CV. Chapters 3.1, 3.2, and 3.3 present studies based on photometric and spectroscopic observations and their aim is to characterise each system. Chapter 3.4 presents a study of a NL system based solely on spectroscopic observation with the objective of analysing the structures of the accretion flow and the accretion disc of the system.

All presented systems can be considered borderline systems, as their mass-transfer rates are close to the critical value that divides stable NLs and unstable DNe, as can be seen in Figure 1.9. CzeV404 Her is an SU UMa type DN, which shows the DN behaviour expected for systems in the unstable branch. The other DN system, AY Psc, is a Z Cam type system, which shows characteristics of both DNe and NLs, suggesting that its mass-transfer rate is just at the border of stability. SDSS1544, a NL system of VY Scl type, exhibits a mass-transfer rate high enough to sustain a stable disc, but not at all times, as it also shows low states during which the disc vanishes. The fourth system, IX Vel, is a NL with a mass-transfer rate at the theoretical border between stable and unstable discs but high enough to sustain a stable disc. However, Kato (2021) hypothesised that IX Vel shows low-amplitude outbursts and that the system is a low-amplitude Z Cam DN alternating between unstable and stable states. Therefore, these four systems present a great opportunity to study CVs with mass-transfer rates close to the critical value dividing stable and unstable discs.

3.1 CzeV404 Her

CzeV404 Her is a DN of SU UMa type which was discovered by Cagas and Cagas (2014). This system was the subject of study by Kára et al. (2021), who characterised the system using light curve modelling and Doppler tomography. The study shows that while CzeV404 Her exhibits outbursts and superoutbursts, which make this DN a SU UMa type system, the structure of the accretion disk resembles a different type of CVs, namely SW Sex-type NLs. This could mean that CzeV404 Her is an evolutionary link between these two types of CVs.

The pages 26–37 are excluded from the online version because their content is protected by copyright. These pages contain a copy of the paper

Kára, J., Zharikov, S., Wolf, M., Kučáková, H., Cagaš, P., Medina Rodriguez, A. L., and Mašek, M. (2021). The period-gap cataclysmic variable CzeV404 Her: A link between SW Sex and SU UMa systems. A&A, 652:A499.

See the attachment No. 1.

3.1.1 CzeV404 Her - recent development

One of the findings reported in Chapter 3.1 is the change of occurrence times of superoutbursts T_{SO} of CzeV404 Her, which changed from $T_{SO} = 142\,d$ to $T_{SO} = 108\,d$, which is behaviour observed also in other SU UMa DN (Vogt, 1980; Vogt et al., 2021). Although the long-term light curve presented by Kára et al. (2021) covers about the next 300 days after the last observed superoutburst, no superoutburst was detected.

Figure 3.1 shows the updated long-term light curve of CzeV404 Her, which extends the covered time span by about 1000 days, and even this light curve does not show any subsequent superoutbursts. There are several outbursts which have

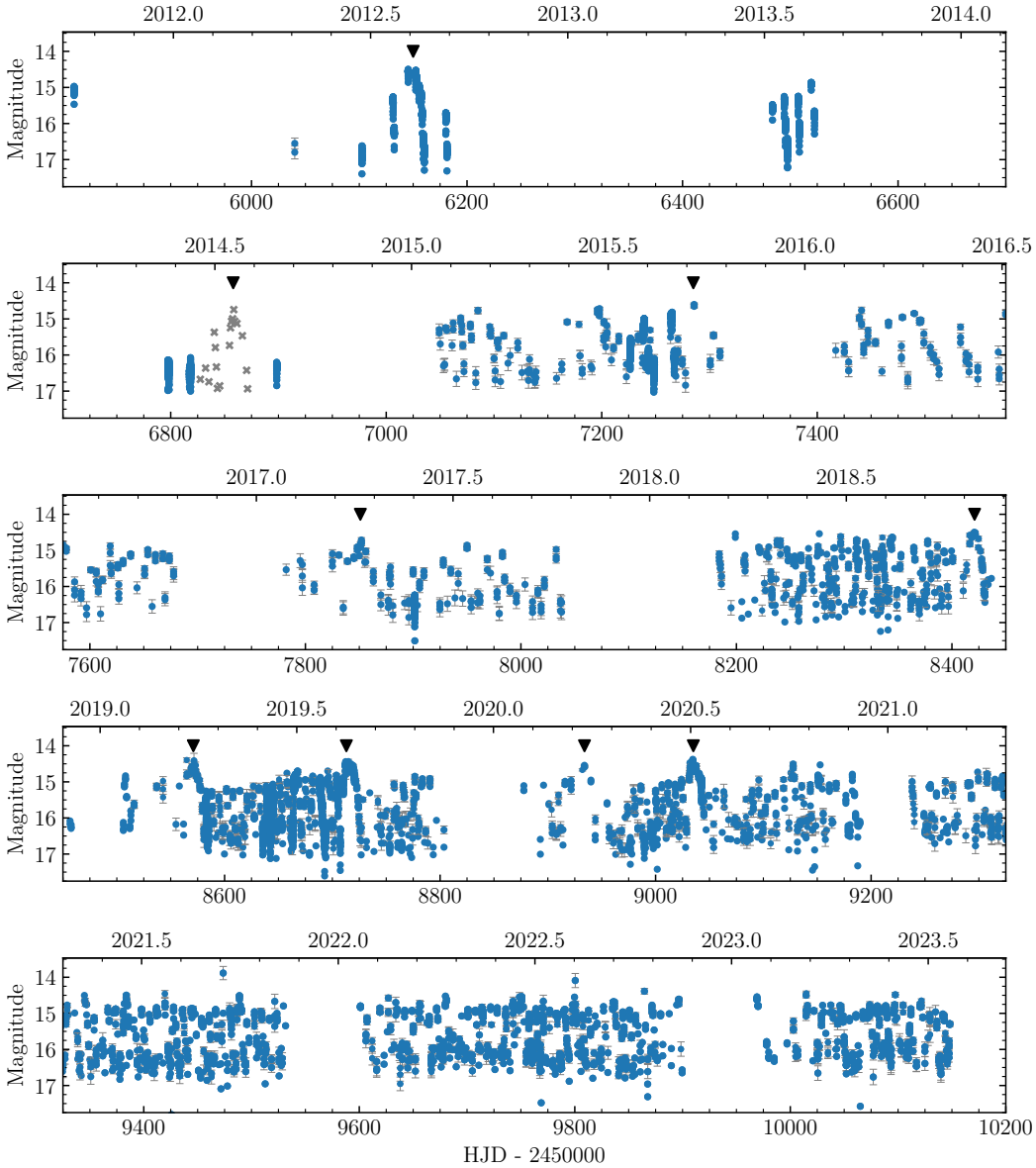

Figure 3.1: Long-term light curve of CzeV404 Her based on data from ASAS-SN survey, ZTF survey, and data obtained at the Ondřejov Observatory and BSO. The grey crosses show the brightest magnitudes of each observational night presented by Bąkowska et al. (2014), the black triangles mark the detected superoutbursts.

amplitude comparable with the amplitude of superoutbursts, but their duration was the same as of normal outbursts. Therefore, it seems that the system has stopped exhibiting super-outbursts. This could indicate that the mass-transfer rate in the system was decreased and nowadays is not high enough to sustain the occurrence of a superoutburst.

If CzeV404 Her truly represents an evolutionary link between SW Sex-type NLs and SU UMa-type DN, as is discussed in Chapter 3.1, one would expect that the system underwent a decrease of its mass-transfer rate. It is possible that the disappearance of superoutbursts is another result of the decrease of mass-transfer rate.

3.2 AY Psc

The CV AY Psc was the subject of study presented by Kára et al. (2023b) who used photometric and spectroscopic observations to characterise the system by modelling the light curve and constructing Doppler maps. AY Psc is a DN of Z Cam-type, which means that the system exhibits two types of activity: active phases, during which the system exhibits DN outbursts, and standstills, during which the system stays in high state similar to NLs. The spectroscopic observation of AY Psc were obtained only during a standstill, and therefore the resulting map can provide us with information about the structure of the accretion disc only during the standstill phase. However, photometric observations were obtained during various stages of activity of this system and they allowed us to study the system in quiescence, standstill, and during an outburst maximum.

The pages 41–59 are excluded from the online version because their content is protected by copyright. These pages contain a copy of the paper

Kára, J., Zharikov, S., Wolf, M., Amantayeva, A., Subebekova, G., Khokhlov, S., Agishev, A., and Merc, J. (2023). The Z Camelopardalis-type Star AY Piscium: Stellar and Accretion Disk Parameters. ApJ, 950, 47.

See the attachment No. 2.

3.3 SDSS J154453.60+255348.8

SDSS1544 is a CV which was found in Sloan Digital Sky Survey (SDSS) by Szkody et al. (2009). The system is an eclipsing NL of the VY Scl-type. This type of NLs, also referred to anti-dwarf novae, is known for its sudden decreases of brightness. SDSS1544 was the subject of study by Medina Rodriguez et al. (2023), who used photometric and spectroscopic observations to characterise the system. The observations were obtained in the high state of this system as well as during an low state, during which no presence of the accretion disc was detected.

The pages 61–74 are excluded from the online version because their content is protected by copyright. These pages contain a copy of the paper

Medina Rodriguez, A. L., Zharikov, S., Kára, J., Wolf, M., Agishev, A. and Khokhlov, S. (2023). VY Scl-type cataclysmic variable SDSS J154453.60+255348.8: stellar and disc parameters. MNRAS, Volume 521, Issue 4, pp.5846-5859.

See the attachment No. 3.

3.4 IX Vel

IX Vel is a non-eclipsing NL discovered by Garrison et al. (1982, 1984) and was subject of numerous studies (e.g. Wargau et al., 1983; Sion, 1985; Haug, 1988; Beuermann and Thomas, 1990; Mauche, 1991; Linnell et al., 2007). Nevertheless, none of these studies employed Doppler tomography to study this system. Kára et al. (2023a) presents a study of IX Vel using Doppler tomography applied to high-resolution spectra. This study uses Balmer lines and helium lines to construct Doppler maps, which show that the emission lines originate dominantly outside of the accretion disc in outflows of the system

The pages 76–89 are excluded from the online version because their content is protected by copyright. These pages contain a copy of the paper

Kára, J., Schmidtobreick, L., Pala, A. F., and Tappert, C. (2023). Structure of the accretion flow of IX Velorum as revealed by high-resolution spectroscopy. A&A, accepted

See the attachment No. 4.

Conclusions

This thesis presents studies of four different CVs, Table 4.1 lists their selected properties, and Figure 4.1 shows the spectral types of their donors and their orbital periods and compares them with other CVs. As can be seen in the table and in the figure, the presented systems have generally diverse properties and they represent different types of CVs. But even though each of these objects belongs to different types and subtypes of CVs, there are several similarities between the systems. As can be seen in Figure 1.9, all four systems can exhibit a mass-transfer rate which is close to the critical value that separates unstable DNe from stable NL. In the case of the two DN systems, CzeV404 Her and AY Psc, this high-mass transfer rate occurs during superoutbursts or outbursts. All of the four studied CVs can be therefore considered good candidates for the study of CVs in the transition region between high-mass transfer NLs and unstable DNe. AY Psc even shows characteristic behaviour of both of these types, with active phases, typical for the DNe, alternating with standstill, during which the system resembles NLs.

The study of these borderline systems can be useful for understanding the evolution of CVs. As Schmidtobreick (2013) pointed out, CVs with orbital period between 2.8 h and 4 h belong almost exclusively to the group of NLs of SW Sex-type, suggesting that SW Sex-type NLs are an evolutionary phase of CVs. As the long-period CVs would evolve towards shorter orbital periods, they would therefore transition between different types as the mass transfer rate would change during their evolution. However, the observed distribution of orbital periods in NLs and DNe contradicts the expected evolutionary behaviour of CVs. Knigge et al. (2011) shows that the mass transfer rate is expected to decrease throughout the evolution of CVs and that a mass transfer rate high enough to sustain a stable disc of NLs can only be expected in long-period systems with $P_{\rm orb} > 5\,{\rm h}$, as can be seen in Figure 1.6. If we assume that NLs with orbital periods in the range between 2.8 h and 4 h became CVs at larger orbital periods and then evolved

Table 4.1: Selected properties of the systems studied in the thesis

System	CzeV404 Her	AY Psc	SDSS1544	IX Vel
Type	SU UMa	Z Cam	VY Scl	NL
$P_{\rm orb}$ [h]	2.35	5.22	6.03	4.65
$M_{\rm WD}$ $[M_\odot]$	1.00(2)	0.90(4)	0.62(7)	0.80(2)
M_2 $[M_\odot]$	0.158	0.45	0.30(4)	0.52(10)
$T_{\rm WD}$ [K]	17 000(5000)	27 600(12 000)	20 500(1000)	60 000(10 000)
T_2 [K]	4100(50)	4100(50)	3400(50)	3500(1000)
$\dot{M}$ $[10^{-10} M_\odot\,{\rm yr}^{-1}]$	0.203(3) 14.6	2.4 15.8 135.7	3.7 – 6.9	50(10)

Notes: The properties of CzeV404 Her, AY Psc, and SDSS1544 were adopted from the studies presented in this thesis. The properties of IX Vel were adopted from the study presented by Linnell et al. (2007). For systems for which mass transfer rates were determined for different states, all determined values are presented in the table.

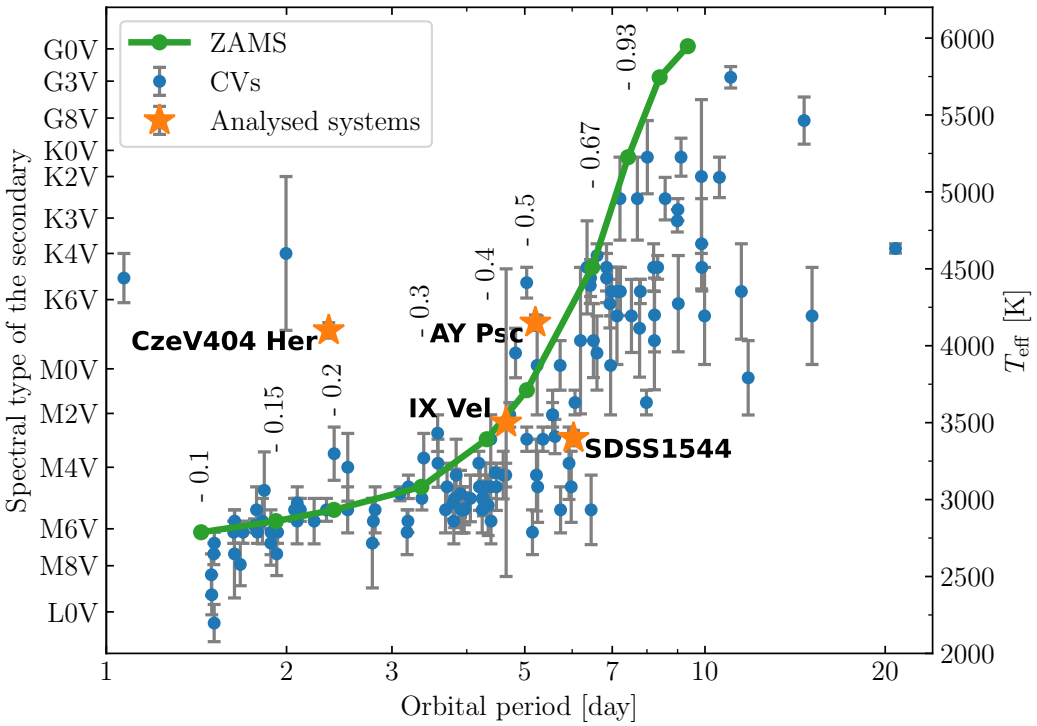

Figure 4.1: Spectral types and effective temperatures of the secondary components of CVs vs. the orbital periods of the systems. The diagram is using updated data from lists presented by Beuermann et al. (1998) and Knigge (2006). The properties of CzeV404 Her, AY Psc, and SDSS1544 were taken from the studies presented in this thesis, the properties of IX Vel were adapted from a study presented by Linnell et al. (2007). The green line shows the properties of CVs with a 0.7 $M_{\odot}$ WD and a main-sequence secondary, the masses of which are labelled in the figure.

to the ones we observe, there needs to be an additional mechanism of angular momentum loss, which is not included in the standard model, and which would increase the mass transfer rates enough to sustain a stable disc observed in NLs.

One of the suggested mechanisms which could increase the angular momentum loss is the outflow of matter from the system, a phenomenon that we detected in AY Psc and IX Vel. Outflows of matter from the accretion disc were observed in many NLs (Tovmassian et al., 2014; Hernandez et al., 2017; Subebekova et al., 2020; Hernández et al., 2021), suggesting that it could be a common phenomenon in these systems. CzeV404 her and SDSS1544 do not show outflows from the accretion disc, but Doppler maps of both systems show that when they are in outburst/high state, the emission lines have a low velocity component, which could be related to winds originating in the accretion disc. While the light curve modelling of SDSS1544 revealed a small accretion disc, and therefore the absence of outflow can be expected, CzeV404 Her shows a large accretion disc extending up to the tidal limitation radius, which would allow outflow to occur. However, as pointed out by Hernandez et al. (2017), emission from the outflow region is expected to be observed in long-period NLs with high mass-transfer rate, and an accretion disc hot enough to produce the observed emission. Systems with a shorter orbital period, lower mass-transfer rate, and a colder disc, on the other

hand, exhibit outflows as an absorption component close to the orbital phase $\varphi = 0.5$. The latter scenario is the case of SW Sex NLs, which show similar structures in Doppler maps as CzeV404. We did not observe such absorption in the case of CzeV404 Her, meaning the presence of an outflow is not supported by the obtained observations.

However, even CzeV404 Her must experience loss of angular momentum through means not included in the standard model of CV evolution, as it is a DN within the period gap. The orbital period of CzeV404 Her $P_{\mathrm{orb}} = 2.35\,\mathrm{h}$ puts the system just above the lower edge of the period gap $P_{\mathrm{gap},-} = 2.15\,\mathrm{h}$. As the value of $P_{\mathrm{gap},-}$ is well defined and consistent within various evolutionary models (Knigge et al., 2011), it is safe to assume that gravitational radiation cannot provide the necessary loss of angular momentum in this system. And the same applies also to other numerous systems located in the period gap, which is populated by DNe and NLs, as can be seen in Figure 1.5

To fully understand the evolution of CVs, it is essential to study the mass transfer in these systems. As the current evolutionary models do not fully explain the observed properties of CVs, studying the systems which contradict the models is important to test new hypotheses. Eclipsing CVs are ideal laboratories for this type of analysis, as they allow us to characterise their properties by light curve modelling and also by Doppler tomography. The study of outflows from the accretion disc of CVs then greatly benefits from high-dispersion spectroscopic observation, which can be used to compute detailed Doppler maps capable of resolving the low-velocity components in these systems.

Bibliography

Amantayeva, A., Zharikov, S., Page, K. L., Pavlenko, E., Sosnovskij, A., Khokhlov, S., and Ibraimov, M. (2021). Period Bouncer Cataclysmic Variable EZ Lyn in Quiescence. *ApJ*, 918(2):58.

Baptista, R. and Bortoletto, A. (2004). Eclipse Mapping of the Flickering Sources in the Dwarf Nova V2051 Ophiuchi. *AJ*, 128(1):411–425.

Baptista, R. and Bortoletto, A. (2008). A Two-armed Pattern in Flickering Maps of the Nova-like Variable UU Aquarii. *ApJ*, 676(2):1240–1247.

Beuermann, K., Baraffe, I., Kolb, U., and Weichhold, M. (1998). Are the red dwarfs in cataclysmic variables main-sequence stars? *A&A*, 339:518–524.

Beuermann, K. and Thomas, H. C. (1990). Detection of emission lines from the secondary star in IX Velorum (=CPD -48 1577). *A&A*, 230:326–338.

Bąkowska, K., Olech, A., Pospieszyński, R., Martinelli, F., and Marciniak, A. (2014). CzeV404 - an Eclipsing Dwarf Nova in the Period Gap During its July 2014 Superoutburst. , 64(4):337–348.

Bruch, A. (2000). Studies of the flickering in cataclysmic variables. VI. The location of the flickering light source in HT Cassiopeiae, V2051 Ophiuchi, IP Pegasi and UX Ursae Majoris. *A&A*, 359:998–1010.

Cagas, P. and Cagas, P. (2014). Discovery of an SU UMa-type eclipsing cataclysmic variable star inside the CV "period gap". *Information Bulletin on Variable Stars*, 6097:1.

Caillault, J.-P. and Patterson, J. (1990). On the Mass-Radius Relation of Late M Dwarfs. *AJ*, 100:825.

Cannizzo, J. K., Still, M. D., Howell, S. B., Wood, M. A., and Smale, A. P. (2010). The Kepler Light Curve of V344 Lyrae: Constraining the Thermal-viscous Limit Cycle Instability. *ApJ*, 725(2):1393–1404.

Clark, D. H. and Stephenson, F. R. (1977). *The historical supernovae.*

Clark, D. H. and Stephenson, F. R. (1982). The Historical Supernovae. In Rees, M. J. and Stoneham, R. J., editors, *Supernovae: A Survey of Current Research*, volume 90 of *NATO Advanced Study Institute (ASI) Series C*, pages 355–370.

Conroy, K. E., Kochoska, A., Hey, D., Pablo, H., Hambleton, K. M., Jones, D., Giammarco, J., Abdul-Masih, M., and Prša, A. (2020). Physics of Eclipsing Binaries. V. General Framework for Solving the Inverse Problem. *ApJS*, 250(2):34.

Dubus, G., Otulakowska-Hypka, M., and Lasota, J.-P. (2018). Testing the disk instability model of cataclysmic variables. *A&A*, 617:A26.

Friend, M. T., Martin, J. S., Smith, R. C., and Jones, D. H. P. (1990). The 8190-A sodium doublet in cataclysmic variables III. Too cool for credibility. *MNRAS*, 246:654.

Garrison, R. F., Hiltner, W. A., and Schild, R. E. (1982). CPD -48 1577. , 3730:2.

Garrison, R. F., Schild, R. E., Hiltner, W. A., and Krzeminski, W. (1984). CPD -48 1577 : the brightest known cataclysmic variable. *ApJ*, 276:L13–L16.

Giovannelli, F. (2008). Cataclysmic Variables: A Review. *Chinese Journal of Astronomy and Astrophysics Supplement*, 8:237–258.

Hameury, J.-M., Menou, K., Dubus, G., Lasota, J.-P., and Hure, J.-M. (1998). Accretion disc outbursts: a new version of an old model. *MNRAS*, 298(4):1048–1060.

Haug, K. (1988). Infrared photometry of the nova-like system IX Velorum (=CPD -48°1577). *MNRAS*, 235:1385–1395.

Hellier, C. (2001). *Cataclysmic Variable Stars*.

Hernández, M. S., Tovmassian, G., Zharikov, S., Gänsicke, B. T., Steeghs, D., Aungwerojwit, A., and Rodríguez-Gil, P. (2021). BG Tri: an example of a low-inclination RW Sex-type nova-like. *MNRAS*, 503(1):1431–1441.

Hernandez, M. S., Zharikov, S., Neustroev, V., and Tovmassian, G. (2017). Structure of accretion flows in nova-like cataclysmic variables: RW Sextantis and 1RXS J064434.5+334451. *MNRAS*, 470(2):1960–1970.

Hessman, F. V. (1987). Accretion Disk Structure in Ss-Cygni. , 130(1-2):351–364.

Hōshi, R. (1979). Accretion Model for Outbursts of Dwarf Nova. *Progress of Theoretical Physics*, 61(5):1307–1319.

Ichikawa, S., Hirose, M., and Osaki, Y. (1993). Superoutburst and Superhump Phenomena in SU Ursae Majoris Stars: Enhanced Mass-Transfer Episode or Pure Disk Phenomenon? , 45:243–253.

Iłkiewicz, K., Scaringi, S., Littlefield, C., and Mason, P. A. (2022). Locating the flickering source in polars. *MNRAS*, 516(4):5209–5215.

Kára, J., Schmidtobreick, L., Pala, A. F., and Tappert, C. (2023a). Structure of the accretion flow of IX Velorum as revealed by high-resolution spectroscopy. *arXiv e-prints*, page arXiv:2308.01102.

Kára, J., Zharikov, S., Wolf, M., Amantayeva, A., Subebekova, G., Khokhlov, S., Agishev, A., and Merc, J. (2023b). The Z Camelopardalis-type Star AY Piscium: Stellar and Accretion Disk Parameters. *ApJ*, 950(1):47.

Kára, J., Zharikov, S., Wolf, M., Kučáková, H., Cagaš, P., Medina Rodriguez, A. L., and Mašek, M. (2021). The period-gap cataclysmic variable CzeV404 Her: A link between SW Sex and SU UMa systems. *A&A*, 652:A49.

Kato, T. (2021). Study of the low-amplitude Z Cam star IX Vel. *arXiv e-prints*, page arXiv:2111.15145.

Kepler, S. O., Kleinman, S. J., Nitta, A., Koester, D., Castanheira, B. G., Giovannini, O., Costa, A. F. M., and Althaus, L. (2007). White dwarf mass distribution in the SDSS. *MNRAS*, 375(4):1315–1324.

Kloppenborg, B. K. (2023). Observations from the aavso international database.

Knigge, C. (2006). The donor stars of cataclysmic variables. *MNRAS*, 373(2):484–502.

Knigge, C., Baraffe, I., and Patterson, J. (2011). The Evolution of Cataclysmic Variables as Revealed by Their Donor Stars. *ApJS*, 194(2):28.

Kochanek, C. S., Shappee, B. J., Stanek, K. Z., Holoien, T. W. S., Thompson, T. A., Prieto, J. L., Dong, S., Shields, J. V., Will, D., Britt, C., Perzanowski, D., and Pojmański, G. (2017). The All-Sky Automated Survey for Supernovae (ASAS-SN) Light Curve Server v1.0. , 129(980):104502.

Kotko, I., Lasota, J. P., Dubus, G., and Hameury, J. M. (2012). Models of AM Canum Venaticorum star outbursts. *A&A*, 544:A13.

Krause, O., Tanaka, M., Usuda, T., Hattori, T., Goto, M., Birkmann, S., and Nomoto, K. (2008). Tycho Brahe's 1572 supernova as a standard typeIa as revealed by its light-echo spectrum. *Nature*, 456(7222):617–619.

Lasota, J. P., Hameury, J. M., and Hure, J. M. (1995). Dwarf novae at low mass transfer rates. *A&A*, 302:L29.

Linnell, A. P., Godon, P., Hubeny, I., Sion, E. M., and Szkody, P. (2007). A Synthetic Spectrum and Light-Curve Analysis of the Cataclysmic Variable IX Velorum. *ApJ*, 662(2):1204–1219.

Linnell, A. P., Godon, P., Hubeny, I., Sion, E. M., and Szkody, P. (2010). The Anomalous Accretion Disk of the Cataclysmic Variable RW Sextantis. *ApJ*, 719(1):271–286.

Longa-Peña, P., Steeghs, D., and Marsh, T. (2015). Emission line tomography of the short period cataclysmic variables CC Scl and V2051 Oph. *MNRAS*, 447(1):149–159.

Marsh, T. R. (2005). Doppler Tomography. , 296(1-4):403–415.

Marsh, T. R. and Horne, K. (1988). Images of accretion discs - II. Doppler tomography. *MNRAS*, 235:269–286.

Masci, F. J., Laher, R. R., Rusholme, B., Shupe, D. L., Groom, S., Surace, J., Jackson, E., Monkewitz, S., Beck, R., Flynn, D., Terek, S., Landry, W., Hacopians, E., Desai, V., Howell, J., Brooke, T., Imel, D., Wachter, S., Ye, Q.-Z., Lin, H.-W., Cenko, S. B., Cunningham, V., Rebbapragada, U., Bue, B., Miller, A. A., Mahabal, A., Bellm, E. C., Patterson, M. T., Jurić, M., Golkhou, V. Z., Ofek, E. O., Walters, R., Graham, M., Kasliwal, M. M., Dekany, R. G.,

Kupfer, T., Burdge, K., Cannella, C. B., Barlow, T., Van Sistine, A., Giomi, M., Fremling, C., Blagorodnova, N., Levitan, D., Riddle, R., Smith, R. M., Helou, G., Prince, T. A., and Kulkarni, S. R. (2019). The Zwicky Transient Facility: Data Processing, Products, and Archive. , 131(995):018003.

Mauche, C. W. (1991). High-Resolution IUE Spectra of the Nova-like Variable IX Velorum. *ApJ*, 373:624.

Medina Rodriguez, A. L., Zharikov, S., Kára, J., Wolf, M., Agishev, A., and Khokhlov, S. (2023). VY Scl-type cataclysmic variable SDSS J154453.60+255348.8: stellar and disc parameters. *MNRAS*, 521(4):5846–5859.

Merc, J., Gális, R., Velez, P., Charbonnel, S., Garde, O., Le Dû, P., Mulato, L., Petit, T., Bohlsen, T., Curry, S., Love, T., and Barker, H. (2023). V618 Sgr: galactic eclipsing symbiotic nova detected in repeated outbursts. *MNRAS*, 523(1):163–168.

Merc, J., Gális, R., and Wolf, M. (2019). First Release of the New Online Database of Symbiotic Variables. *Research Notes of the American Astronomical Society*, 3(2):28.

Neustroev, V. V., Marsh, T. R., Zharikov, S. V., Knigge, C., Kuulkers, E., Osborne, J. P., Page, K. L., Steeghs, D., Suleimanov, V. F., Tovmassian, G., Breedt, E., Frebel, A., García-Díaz, M. T., Hambsch, F. J., Jacobson, H., Parsons, S. G., Ryu, T., Sabin, L., Sjoberg, G., Miroshnichenko, A. S., Reichart, D. E., Haislip, J. B., Ivarsen, K. M., LaCluyze, A. P., and Moore, J. P. (2017). The remarkable outburst of the highly evolved post-period-minimum dwarf nova SSS J122221.7-311525. *MNRAS*, 467(1):597–618.

Osaki, Y. (1985). Irradiation-induced mass-overflow instability as a possible cause of superoutbursts in SU UMa stars. *A&A*, 144:369–380.

Osaki, Y. (1989). A model for the superoutburst phenomenon of SU Ursae MAjoris stars. , 41:1005–1033.

Osaki, Y. (2005). The disk instability model for dwarf nova outbursts. *Proceedings of the Japan Academy, Series B*, 81:291–305.

Otulakowska-Hypka, M., Olech, A., and Patterson, J. (2016). Statistical analysis of properties of dwarf novae outbursts. *MNRAS*, 460(3):2526–2541.

Pala, A. F., Gänsicke, B. T., Belloni, D., Parsons, S. G., Marsh, T. R., Schreiber, M. R., Breedt, E., Knigge, C., Sion, E. M., Szkody, P., Townsley, D., Bildsten, L., Boyd, D., Cook, M. J., De Martino, D., Godon, P., Kafka, S., Kouprianov, V., Long, K. S., Monard, B., Myers, G., Nelson, P., Nogami, D., Oksanen, A., Pickard, R., Poyner, G., Reichart, D. E., Rodriguez Perez, D., Shears, J., Stubbings, R., and Toloza, O. (2022). Constraining the evolution of cataclysmic variables via the masses and accretion rates of their underlying white dwarfs. *MNRAS*, 510(4):6110–6132.

Pala, A. F., Schmidtobreick, L., Tappert, C., Gänsicke, B. T., and Mehner, A. (2018). The cataclysmic variable QZ Lib: a period bouncer. *MNRAS*, 481(2):2523–2535.

Patterson, J. (1984). The evolution of cataclysmic and low-mass X-ray binaries. *ApJS*, 54:443–493.

Patterson, J. (2011). Distances and absolute magnitudes of dwarf novae: murmurs of period bounce. *MNRAS*, 411(4):2695–2716.

Pilarčík, L., Wolf, M., Dubovský, P. A., Hornoch, K., and Kotková, L. (2012). Period changes of the long-period cataclysmic binary EX Draconis. *A&A*, 539:A153.

Pilarčík, L., Wolf, M., Zasche, P., and Vraštil, J. (2018). Period changes of cataclysmic variables below the period gap: V2051 Oph, OY Car and Z Cha. , 60:1–6.

Pojmanski, G. (1997). The All Sky Automated Survey. , 47:467–481.

Politano, M. (1996). Theoretical Statistics of Zero-Age Cataclysmic Variables. *ApJ*, 465:338.

Prša, A., Conroy, K. E., Horvat, M., Pablo, H., Kochoska, A., Bloemen, S., Giammarco, J., Hambleton, K. M., and Degroote, P. (2016). Physics Of Eclipsing Binaries. II. Toward the Increased Model Fidelity. *ApJS*, 227(2):29.

Prša, A. and Zwitter, T. (2005). A Computational Guide to Physics of Eclipsing Binaries. I. Demonstrations and Perspectives. *ApJ*, 628(1):426–438.

Rappaport, S., Joss, P. C., and Webbink, R. F. (1982). The evolution of highly compact binary stellar systems. *ApJ*, 254:616–640.

Ratering, C., Bruch, A., and Diaz, M. (1993). A spectroscopic study of the Z Camelopardalis type dwarf nova KT Persei. *A&A*, 268:694–704.

Ricker, G. R., Winn, J. N., Vanderspek, R., Latham, D. W., Bakos, G. Á., Bean, J. L., Berta-Thompson, Z. K., Brown, T. M., Buchhave, L., Butler, N. R., Butler, R. P., Chaplin, W. J., Charbonneau, D., Christensen-Dalsgaard, J., Clampin, M., Deming, D., Doty, J., De Lee, N., Dressing, C., Dunham, E. W., Endl, M., Fressin, F., Ge, J., Henning, T., Holman, M. J., Howard, A. W., Ida, S., Jenkins, J., Jernigan, G., Johnson, J. A., Kaltenegger, L., Kawai, N., Kjeldsen, H., Laughlin, G., Levine, A. M., Lin, D., Lissauer, J. J., MacQueen, P., Marcy, G., McCullough, P. R., Morton, T. D., Narita, N., Paegert, M., Palle, E., Pepe, F., Pepper, J., Quirrenbach, A., Rinehart, S. A., Sasselov, D., Sato, B., Seager, S., Sozzetti, A., Stassun, K. G., Sullivan, P., Szentgyorgyi, A., Torres, G., Udry, S., and Villasenor, J. (2014). Transiting Exoplanet Survey Satellite (TESS). In Oschmann, Jacobus M., J., Clampin, M., Fazio, G. G., and MacEwen, H. A., editors, *Space Telescopes and Instrumentation 2014: Optical, Infrared, and Millimeter Wave*, volume 9143 of *Society of Photo-Optical Instrumentation Engineers (SPIE) Conference Series*, page 914320.

Ritter, H. and Kolb, U. (2003). Catalogue of cataclysmic binaries, low-mass X-ray binaries and related objects (Seventh edition). *A&A*, 404:301–303.

Ritter, H. and Kolb, U. (2004). VizieR Online Data Catalog: Cataclysmic Binaries, LMXBs, and related objects (Ritter+, 2003). *VizieR Online Data Catalog*, page V/113C.

Ritter, H. and Kolb, U. (2011). VizieR Online Data Catalog: Cataclysmic Binaries, LMXBs, and related objects (Ritter+, 2004). *VizieR Online Data Catalog*, page B/cb.

Robinson, E. L. (1976). The structure of cataclysmic variables. , 14:119–142.

Salazar, I. V., LeBleu, A., Schaefer, B. E., Landolt, A. U., and Dvorak, S. (2017). Accurate pre- and post-eruption orbital periods for the dwarf/classical nova V1017 Sgr. *MNRAS*, 469(4):4116–4132.

Scaringi, S., Groot, P. J., Knigge, C., Bird, A. J., Breedt, E., Buckley, D. A. H., Cavecchi, Y., Degenaar, N. D., de Martino, D., Done, C., Fratta, M., Iłkiewicz, K., Koerding, E., Lasota, J. P., Littlefield, C., Manara, C. F., O'Brien, M., Szkody, P., and Timmes, F. X. (2022a). Localized thermonuclear bursts from accreting magnetic white dwarfs. *Nature*, 604(7906):447–450.

Scaringi, S., Groot, P. J., Knigge, C., Lasota, J. P., de Martino, D., Cavecchi, Y., Buckley, D. A. H., and Camisassa, M. E. (2022b). Triggering micronovae through magnetically confined accretion flows in accreting white dwarfs. *MNRAS*, 514(1):L11–L15.

Schmidtobreick, L. (2013). The SW Sex Phenomenon as an Evolutionary Stage of Cataclysmic Variables. *Central European Astrophysical Bulletin*, 37:361–368.

Schmidtobreick, L., Shara, M., Tappert, C., Bayo, A., and Ederoclite, A. (2015). On the absence of nova shells. *MNRAS*, 449(2):2215–2218.

Schneider, D. P. and Young, P. (1980). The magnetic maw of 2A 0311-22.7. *ApJ*, 238:946–954.

Schreiber, M. R., Hameury, J. M., and Lasota, J. P. (2004). Delays in dwarf novae II: VW Hyi, the tidal instability and enhanced mass transfer models. *A&A*, 427:621–635.

Schreiber, M. R., Zorotovic, M., and Wijnen, T. P. G. (2016). Three in one go: consequential angular momentum loss can solve major problems of CV evolution. *MNRAS*, 455(1):L16–L20.

Shafter, A. W. (1983). Radial velocity studies of cataclysmic binaries. I. KR Aurigae. *ApJ*, 267:222–231.

Shappee, B. J., Prieto, J. L., Grupe, D., Kochanek, C. S., Stanek, K. Z., De Rosa, G., Mathur, S., Zu, Y., Peterson, B. M., Pogge, R. W., Komossa, S., Im, M., Jencson, J., Holoien, T. W. S., Basu, U., Beacom, J. F., Szczygieł, D. M., Brimacombe, J., Adams, S., Campillay, A., Choi, C., Contreras, C., Dietrich, M., Dubberley, M., Elphick, M., Foale, S., Giustini, M., Gonzalez, C., Hawkins, E., Howell, D. A., Hsiao, E. Y., Koss, M., Leighly, K. M., Morrell, N., Mudd, D., Mullins, D., Nugent, J. M., Parrent, J., Phillips, M. M., Pojmanski, G.,

Rosing, W., Ross, R., Sand, D., Terndrup, D. M., Valenti, S., Walker, Z., and Yoon, Y. (2014). The Man behind the Curtain: X-Rays Drive the UV through NIR Variability in the 2013 Active Galactic Nucleus Outburst in NGC 2617. *ApJ*, 788(1):48.

Shara, M. M., Iłkiewicz, K., Mikołajewska, J., Pagnotta, A., Bode, M. F., Crause, L. A., Drozd, K., Faherty, J., Fuentes-Morales, I., Grindlay, J. E., Moffat, A. F. J., Pretorius, M. L., Schmidtobreick, L., Stephenson, F. R., Tappert, C., and Zurek, D. (2017). Proper-motion age dating of the progeny of Nova Scorpii AD 1437. *Nature*, 548(7669):558–560.

Shara, M. M., Prialnik, D., Hillman, Y., and Kovetz, A. (2018). The Masses and Accretion Rates of White Dwarfs in Classical and Recurrent Novae. *ApJ*, 860(2):110.

Sion, E. M. (1985). On the nature of the UX Ursa Majoris-type nova-like variables : CPD -48 1577. *ApJ*, 292:601–605.

Skottfelt, J., Bramich, D. M., Hundertmark, M., Jørgensen, U. G., Michaelsen, N., Kjærgaard, P., Southworth, J., Sørensen, A. N., Andersen, M. F., Andersen, M. I., Christensen-Dalsgaard, J., Frandsen, S., Grundahl, F., Harpsøe, K. B. W., Kjeldsen, H., and Pallé, P. L. (2015). The two-colour EMCCD instrument for the Danish 1.54 m telescope and SONG. *A&A*, 574:A54.

Smak, J. (1984). Accretion in cataclysmic binaries. IV. Accretion disks in dwarf novae. , 34:161–189.

Smak, J. (2008). Superoutbursts of Z Cha and their Interpretation. , 58:55–64.

Smak, J. (2009a). Are Disks in Dwarf Novae during their Superoutbursts Really Eccentric? , 59(1):89–101.

Smak, J. (2009b). New Interpretation of Superhumps. , 59(1):121–130.

Smak, J. (2009c). On the Amplitudes of Superhumps. , 59(1):103–107.

Smak, J. (2009d). Z Cha and its Superhumps. , 59(1):109–120.

Southworth, J., Hickman, R. D. G., Marsh, T. R., Rebassa-Mansergas, A., Gänsicke, B. T., Copperwheat, C. M., and Rodríguez-Gil, P. (2009). Orbital periods of cataclysmic variables identified by the SDSS. VI. The 4.5-h period eclipsing system SDSS J100658.40+233724.4. *A&A*, 507(2):929–937.

Spruit, H. C. (1998). Fast maximum entropy Doppler mapping. *arXiv e-prints*, pages astro–ph/9806141.

Spruit, H. C. (2021). dopmap: Fast Doppler mapping program. Astrophysics Source Code Library, record ascl:2106.002.

Stephenson, F. R. and Clark, D. H. (1976). Historical supernovas. *Scientific American*, 234:100–107.

Subebekova, G., Zharikov, S., Tovmassian, G., Neustroev, V., Wolf, M., Hernandez, M. S., Kučáková, H., and Khokhlov, S. (2020). Structure of accretion flows in the nova-like cataclysmic variable RW Tri. *MNRAS*, 497(2):1475–1487.

Szkody, P., Anderson, S. F., Hayden, M., Kronberg, M., McGurk, R., Riecken, T., Schmidt, G. D., West, A. A., Gänsicke, B. T., Nebot Gomez-Moran, A., Schneider, D. P., Schreiber, M. R., and Schwope, A. D. (2009). Cataclysmic Variables from SDSS. VII. The Seventh Year (2006). *AJ*, 137(4):4011–4019.

Tappert, C., Mennickent, R. E., Arenas, J., Matsumoto, K., and Hanuschik, R. W. (2003). An atlas of line profile studies for SU UMa type cataclysmic variables. *A&A*, 408:651–661.

Thoroughgood, T. D., Dhillon, V. S., Littlefair, S. P., Marsh, T. R., and Smith, D. A. (2001). The mass of the white dwarf in the recurrent nova U Scorpii. *MNRAS*, 327(4):1323–1333.

Tovmassian, G., Stephania Hernandez, M., González-Buitrago, D., Zharikov, S., and García-Díaz, M. T. (2014). On the SW Sex-type Eclipsing Cataclysmic Variable SDSS0756+0858. *AJ*, 147(3):68.

Uthas, H., Knigge, C., Long, K. S., Patterson, J., and Thorstensen, J. (2011). The cataclysmic variable SDSS J1507+52: an eclipsing period bouncer in the Galactic halo. *MNRAS*, 414(1):L85–L89.

Vogt, N. (1980). The SU UMa stars, an important sub-group of dwarf novae. *A&A*, 88:66–76.

Vogt, N. (1983). VW Hydri revisited : conclusions on dwarf nova outburst models. *A&A*, 118:95–101.

Vogt, N., Puebla, E. C., and Contreras-Quijada, A. (2021). Determination of the superoutburst cycle lengths of 206 SU UMa-type dwarf novae. *MNRAS*, 502(4):5668–5678.

Wade, R. A. and Horne, K. (1988). The Radial Velocity Curve and Peculiar TiO Distribution of the Red Secondary Star in Z Chamaeleontis. *ApJ*, 324:411.

Wargau, W., Drechsel, H., Rahe, J., and Bruch, A. (1983). Spectrophotometry of the recently discovered cataclysmic variable CPD -48 1577. *MNRAS*, 204:35P–39.

Warner, B. (1995). *Cataclysmic variable stars*, volume 28.

Whitehurst, R. (1988). Numerical simulations of accretion discs - I. Superhumps : a tidal phenomenon of accretion discs. *MNRAS*, 232:35–51.

Wilson, R. E. and Devinney, E. J. (1971). Realization of Accurate Close-Binary Light Curves: Application to MR Cygni. *ApJ*, 166:605.

Yaron, O., Prialnik, D., Shara, M. M., and Kovetz, A. (2005). An Extended Grid of Nova Models. II. The Parameter Space of Nova Outbursts. *ApJ*, 623(1):398–410.

Zangrilli, L., Tout, C. A., and Bianchini, A. (1997). How two Cohabiting Magnetic Dynamos explain the Secular Evolution of Cataclysmic Variables. *MNRAS*, 289(1):59–65.

Zharikov, S., Tovmassian, G., Aviles, A., Michel, R., Gonzalez-Buitrago, D., and García-Díaz, M. T. (2013). The accretion disk in the post period-minimum cataclysmic variable SDSS J080434.20 + 510349.2. *A&A*, 549:A77.

Zorotovic, M. and Schreiber, M. R. (2020). Cataclysmic variable evolution and the white dwarf mass problem: A Review. *Advances in Space Research*, 66(5):1080–1089.

List of Figures

List of Abbreviations

AAVSO	American Association of Variable Star Observers
ASAS	All-Sky Automated Survey
ASAS-SN	All-Sky Automated Survey for Supernovae
CV	Cataclysmic variable
D65	Mayer 0.65-m telescope
DK154	Danish 1.54-m telescope
DN	Dwarf nova
ESO	European Southern Observatory
IR	Infrared
NL	Nova-like
OAN	Observatorio Astronómico Nacional
SPM	San Pedro Mártir Observatory
TESS	Transiting Exoplanet Survey Satellite
UV	Ultraviolet
ZAMS	Zero-age main sequence
ZTF	Zwicky Transient Facility

List of publications

In the chronological order:

Zasche, P., Vokrouhlický, D., Wolf, M., Kučáková, H., **Kára, J.**, Uhlař, R., Mašek, M., Henzl, Z., & Cagaš, P. (2019). *Doubly eclipsing systems.* A&A 630, A128.

Hornoch, K., Carey, G., Kucakova, H., & **Kara, J.** (2019). *Discovery of a Possible Nova in M31.* The Astronomer's Telegram 13198, 1.

Zasche, P., Wolf, M., Kučáková, H., **Kára, J.**, Merc, J., Zejda, M., Skarka, M., Janík, J., & Kurfürst, P. (2020). *First apsidal motion and light curve analysis of 162 eccentric eclipsing binaries from LMC.* A&A 640, A33.

Merc, J., Gális, R., **Kára, J.**, Wolf, M., & Vrašťák, M. (2020). *The nature of the symbiotic candidate 2MASS J07363415+6538548 in the field of NGC 2403.* MNRAS 499, 2116-2123.

Wolf, M., Kučáková, H., Zasche, P., Hornoch, K., **Kára, J.**, Merc, J., & Zejda, M. (2021). *Possible substellar companions in dwarf eclipsing binaries. SDSS J143547.87+373338.5, NSVS 7826147, and NSVS 14256825.* A&A 647, A65.

Kára, J., Zharikov, S., Wolf, M., Kučáková, H., Cagaš, P., Medina Rodriguez, A. L., & Mašek, M. (2021). *The period-gap cataclysmic variable CzeV404 Her: A link between SW Sex and SU UMa systems.* A&A 652, A49.

Zasche, P., Henzl, Z., & **Kára, J.** (2022). *The first study of four doubly eclipsing systems.* A&A 659, A8.

Hornoch, K., Scheirich, P., Srba, J., Skarka, M., Fatka, P., Henych, T., Pavelka, J., **Kara, J.**, Kucakova, H., & Shafter, A. W. (2023). *Discovery of a Probable Nova in M31.* The Astronomer's Telegram 15965, 1.

Šmelcer, L., Wolf, M., Kučáková, H., Zasche, P., **Kára, J.**, Hornoch, K., Zejda, M., & Auer, R. F. (2023). *A photometric study of NSVS 7453183: a probable quadruple system with long-term surface activity.* MNRAS 520, 353-363.

Medina Rodriguez, A. L., Zharikov, S., **Kára, J.**, Wolf, M., Agishev, A., & Khokhlov, S. (2023). *VY Scl-type cataclysmic variable SDSS J154453.60+255348.8: stellar and disc parameters.* MNRAS 521, 5846-5859.

Kára, J., Zharikov, S., Wolf, M., Amantayeva, A., Subebekova, G., Khokhlov, S., Agishev, A. and Merc, J. (2023). *The Z Camelopardalis-type Star AY Piscium: Stellar and Accretion Disk Parameters.* ApJ, 950, 47.

Merc, J., Gális, R., Wolf, M., Dubovský, P. A., **Kára, J.**, Sims, F., Foster, J. R., Medulka, T., Boussin, C., Coffin, J. P., Buil, C., Boyd, D., & Montier, J. (2023). *Comprehensive analysis of a symbiotic candidate V503 Her.* AJ, 166, 65.

Kára, J., Schmidtobreick, L., Pala, A. F., & Tappert, C. (2023). *Structure of the accretion flow of IX Velorum as revealed by high-resolution spectroscopy.* A&A, accepted